5-2021

A Laboratory Study on the Geometric Effects of Piano Key Weirs on Scour for Non-Cohesive Substrates and Simple Mitigation Techniques

Wyatt Lantz
Utah State University

A LABORATORY STUDY ON THE GEOMETRIC EFFECTS OF PIANO KEY WEIRS ON SCOUR FOR NON-COHESIVE SUBSTRATES AND SIMPLE MITIGATION TECHNIQUES

by

Wyatt Lantz

A thesis submitted in partial fulfillment
of the requirements for the degree

of

MASTER OF SCIENCE

in

Civil and Environmental Engineering

Approved:

_____	_____
Brian M. Crookston, Ph.D., P.E. Major Professor	Blake P. Tullis, Ph.D. Committee Member
_____	_____
Austin Ball, M.S., S.E. Committee Member	D. Richard Cutler, Ph.D. Interim Vice Provost for Graduate Studies

UTAH STATE UNIVERSITY
Logan, Utah

2021

ABSTRACT

A Laboratory Study of the Geometric Effects of Piano Key Weirs on Scour for a Non-Cohesive Substrates and Simple Mitigation Techniques

by

Wyatt Lantz, Master of Science

Utah State University, 2021

Major Professor: Dr. Brian M. Crookston
Department: Civil and Environmental Engineering

Sustainable flood control infrastructure is needed as climate change continues to produce more extreme precipitation events, as water infrastructure continues to age, and as populations continue to grow and expand. Weirs, particularly non-linear weirs such as labyrinth and piano key weirs, are sustainable passive flood-control structures being considered for rehabilitation and new projects due to their improved hydraulic performance, low maintenance, and construction costs. However, like other structures, these weirs are susceptible to local scour if the foundation remains unprotected. The scour phenomenon is a complicated process dependent upon multiple variables. Despite extensive research on scour, there is limited information for non-linear weirs with little directed to practitioners attempting to design scour protection measures for these structures. Due to this lack of information, a large-scale laboratory study is performed to consider scour morphology and evolution, scour prediction, and scour mitigation

techniques that could be employed by practitioners. The limitations of this study include the discharges, headwaters, and tailwaters tested for two non-cohesive gravel substrates. Scour intensity, the time needed to reach equilibrium, and scour morphology are dependent upon hydraulic conditions. Published scour prediction equations are evaluated to determine the relative accuracy in estimating maximum geometric scour features at piano key weirs. Using published scour prediction equations, new scour mitigation design equations are generated to assist practitioners in the selection of apron lengths and cutoff wall depths for piano key weirs. It is determined that an apron 1.5 times the weir height is an optimal apron length to minimize scour by, on average, 75%.

(107 Pages)

PUBLIC ABSTRACT

A Laboratory Study of the Geometric Effects of Piano Key Weirs on Scour for Non-Cohesive Substrates and Simple Mitigation Techniques

Wyatt Lantz

Sustainable flood control infrastructure is needed as climate change continues to produce more extreme precipitation events, as our water infrastructure continues to age, and as populations continue to grow and expand. Non-linear weirs, such as labyrinth and piano key weirs, are sustainable passive flood-control structures due to their improved hydraulic performance, and low maintenance and construction costs. However, like other structures, these weirs are susceptible to local scour, which is removal of soil and rock due to hydraulic forces. The scour phenomenon is a complicated process dependent upon multiple variables. There is limited information for non-linear weirs with little directed to practitioners attempting to design scour protection measures for these structures. Due to this lack of information, a laboratory study is performed to consider scour morphology and evolution, scour prediction, and scour mitigation techniques that could be employed by practitioners. Hydraulic conditions affect the scour intensity, the time it takes to reach equilibrium, and the overall scour morphology. Published scour prediction equations are evaluated to determine the relative accuracy in estimating maximum geometric scour features at piano key weirs. Using published scour prediction equations, new scour mitigation design equations are generated to assist practitioners in the development of aprons lengths and cutoff wall depths for piano key weirs.

ACKNOWLEDGMENTS

I am grateful for the opportunity that I have had to work at the Utah Water Research Laboratory and to have been taught and surrounded by some of the leading experts in the field of civil engineering. This is an exceptional facility ran by individuals who care about the advancement of technology in civil engineering and who want to give the rising generation of engineers all the knowledge that they have.

I want to thank the Crookston team for always helping me collect data, start experimental runs, and shovel gravel. I am particularly thankful for the help and support that I received from Shelby Bulkley, Taylor Shapiro, and Kade Flake. Shelby watched the almost endless hours of experimental videos and helped me collect data for the study. Taylor helped me with data entry, coding guidance, and replacing the gravel. Lastly, Kade has been there for me through the unfair tests and has talked me off the ledge on quitting days.

I am grateful to my committee for their support and mentorship as I prepared my thesis. I'm thankful for Professor Ball being willing to be on my committee and for his excellent instruction through my undergraduate degree. I am grateful for Dr. Tullis being willing to be on my committee and for his love for hydraulics, it is inspiring to me. I would particularly like to give Dr. Crookston thanks for hiring me at the UWRL. I am grateful for all the help that he has given to me during this project and his ambition to help me receive funding for the project. I am also thankful for the mentoring that I have received from him to prepare me to work in industry. I am grateful that he took the chance on me and I hope that I have not let him down in any way. Dr. Crookston, your insane work ethic and love for what you do inspires me to do my best.

Last and far from least is the great thanks I have for my family, and I have a large family. I am thankful to the Lantz's, Call's (loving adopted family), and Olsen's for all their loving support. I know that I have not been the most engaged the last few years, but I want them to know that I do love each one of them, and I am thankful for their calls, texts, and family parties. Most importantly, I am thankful for my wife, Kayla. I am thankful that she was willing to put her education on hold to support us financially through this endeavor. I am thankful that I have her emotional support and the opportunity to come home to her every night and be able to talk through stresses and frustrations. I am thankful that she is willing to support me in my career and go where ever life takes us. I know, that I could not have married a better woman. Kayla, I love you now and always. Thank you for all the help.

- Wyatt Lantz

CONTENTS

Page

Abstract iii

Public Abstract v

Acknowledgments vi

List Of Tables x

List Of Figures xi

Nomenclature xiv

Introduction 1

Experimental Setup 4

Testing Facilities 4
Physical Model 5
Instrumentation 9

Methodology 13

Piano Key Weir Geometric Effects on Scour Morphology 13
Apron and Cutoff Wall Design Study 14

Evolution of Local Scour Downstream of a Type A PK Weir in Non-Cohesive Sediments 16

Abstract 16
Introduction 16
Experimental Setup 20

Facility 20
Substrate 22
Instrumentation 23
Testing Scheme 25
Testing Methodology 26

Results 26

Scour-inducing PK Weir Hydraulics 26
Temporal Evolution 27

Graphical Prediction of PK Weir Scour 30
Maximum Scour Prediction 35

Conclusions 40

Apron and Cutoff Wall Scour Protection for Piano Key Weirs 43

Abstract 43
Introduction 43
Experimental Setup 46
Results 50

Hydraulic Observations 50
Local Scour 51
Horizontal Apron Design Guidance 55
Cutoff Wall Design 57

Conclusions 58

Conclusions 60

References 62

Appendices 70

Appendix A – USU Custom MATLAB Script 71
Appendix B – Flume Design Drawings 88

LIST OF TABLES

Page

Table 1– PK weir parameters. 7

Table 2 – Substrate granulometric properties. 8

Table 3 – x_{mi} location based on substrate material. 11

Table 4 – Intel RealSense D435 depth camera features. 12

Table 5 – Test matrix for the PK weir geometric effects on scour morphology study. 13

Table 6 – Test matrix for the apron and cutoff wall design study. 15

Table 7 – Geometric parameters of the PK weir. 21

Table 8 – Granulometric properties of the substrate materials. 22

Table 9 – Test matrix for study. 25

Table 10 – Maximum scour parameters from each experimental run, where xR specifies a rerun for that experimental run. 31

Table 11 – Experimental PK dimension summary. 48

Table 12 – Intel RealSense D435 specifications. 50

Table 13 – Test matrix for the current study for the coarse and fine substrate. 50

Table 14 – Testing values for each experimental run. 53

Table 15 – Measured experimental values. 54

LIST OF FIGURES

Page

Fig. 1. Plan view of flume, baffle wall, stilling well tap, weir, scour box, and stop log assembly.....5

Fig. 2. Photograph of the flume in the UWRL. 5

Fig. 3. Hydraulic schematic for the study. 6

Fig. 4. Geometric schematic of PK weir and apron setup. 6

Fig. 5. Sieve analysis for the two-substrate material. 8

Fig 6. Substrate material comparisons. 9

Fig. 7. 30.5 cm (a) and 61 cm (b) diameter supply lines with butterfly control valves (1), pressure transducer (2), multimeter (3), Hart communicator sensor (4), and Venturi meter pressure taps (5). 10

Fig. 8. Sphere animation as scour occurs. 11

Fig. 9. Illustration of experimental setup with PK geometry and scour morphology. 20

Fig. 10. Geometric and hydraulic parameters of this study. 21

Fig. 11. Sieve analysis for substrate material. 23

Fig. 12. Controlled specific weight of spheres minimize premature evacuation from substrate.....24

Fig. 13. Three-dimensional jet patterns produced by PK weir. 27

Fig. 14. Channel view of PK weir.....27

Fig 15A-C. Scour development with time for (A) Initial Phase, (B) Second Phase, and (C) Final Phase (timer displays time of observation).....28

Fig. 16A and B. Sieve analysis of the bed material from the upstream slope of the scour hole and the max scour location, where (A) represents coarse substrate and (B) fine substrate material.....29

Fig. 17A and B. Maximum scour profiles for (A) coarse substrate and (B) fine substrate material. Table 10 can be used as a reference for hydraulic conditions and scour features. 30

Fig. 18A and B. Tailwater to maximum scour rating curves (A) coarse substrate and (B) fine substrate material. 32

Fig. 19A-D. Observed scour depth with time (to 360 min) (A and C) and scour length with time (to 360 min) (B and D) for each flowrate material. Where A and B represent the coarse substrate and C and D represent the fine substrate. The most dramatic scour in both substrates occurs within the first 100 min of experimentation....34

Fig. 20A and B. Time evolution prediction using Nasrollahi et al. (2008) method for (A.) coarse substrate and (B.) fine substrate. 35

Fig. 21. General trend of K_l versus ΔH with a general trendline. 37

Fig. 22. Comparison of various literature prediction methods and actual measured values. 40

Fig. 23. Plan and profile view of weir dimensions and flume set up....47

Fig. 24. Profile of experimental setup with key parameters used in this study. 48

Fig. 25A and B. Run 14 (A) in comparison to Run 23 (B) for the fine substrate, Q =300 l/s, and h_d = 0.17 m (Table 4). Run 23 has significantly less scour due to L_a = 2.0P. 51

Fig. 26A and B. 2D maximum scour profiles for various L_a and Q for (A) the coarse substrate and (B) fine substrate. Run numbers are associated with Table 14. Note that the sediment bed was deeper than 1 m. 52

Fig. 27A and B. Reduction in scour with increased L_a for (A) coarse substrate and (B) fine substrate. 52

Fig. 28A and B. A graphical view of the effects L_a has on Z_{max} for (A) coarse substrate and (B) fine substrate. 55

Fig. 29A and B. A graphical view of the effects L_a has on the L_{max} for (A) coarse substrate and (B) fine substrate. 55

Fig 30. Predicted Z_{max} plotted against observed Z_{max} downstream of L_a. 57

Fig. 31. Scour mitigation options. 58

Fig. B1. Flume plan view dimensions. 89

Fig. B2. Profile view of flume with dimensions. 90

Fig. B3. Schematic of PK weir with dimensions. 91

NOMENCLATURE

a	empirical constant in Nasrollahi et al. (2008) method;
a_m	empirical coefficient in Mason and Arumugam (1985) method;
B	depth of PK weir in streamwise direction (m);
B_b	depth of PK weir base in streamwise direction (m);
B_i	depth of PK weir inlet key overhang in streamwise direction (m);
B_o	depth of PK weir outlet key overhang in streamwise direction (m);
b	empirical constant in Nasrollahi et al. (2008) method;
c	empirical coefficient in Mason and Arumugam (1985) method;
d_{50}	fifty percent of the material is finer (m);
d_{90}	ninety percent of the material is finer (m);
e	empirical coefficient in Mason and Arumugam (1985) method;
Fr_{sd}	densimetric Froude number;
$F.S.$	factor of safety;
f	constant empirical coefficient in current study;
G	specific gravity of substrate material;
g	gravitational constant (m/s^2);
H	total head (m);
H_d	downstream head, $h_d + V^2/2g$ (m);
H_u	upstream head, $H+P$ (m);
ΔH	change in energy head upstream to downstream (m);
h_c	critical depth (m);
h_d	tailwater depth or piezometric head of water downstream of the weir (m);

h_u	piezometric head of water upstream of the weir (m);
K	empirical coefficient in Mason and Arumugam (1985) method;
K_b	empirical coefficient in Bormann and Julien (1991) method;
K_l	empirical coefficient in current study;
k	empirical coefficient in Mason and Arumugam (1985) method;
L	maximum scour hole length (m);
L_a	apron length (m);
L_c	length or depth of cutoff wall (m);
L_{design}	chosen apron design length (m);
L_{max}	maximum scour hole length (m);
L_{pre}	predicted apron length (m);
m	constant empirical coefficient in current study;
N	number of PK weir cycles;
n	empirical coefficient in Mason and Arumugam (1985) method;
P	weir height (m);
P_d	Piano Key foundation height (m);
p	constant empirical coefficient in current study;
Q	flow rate or volumetric discharge (m^3/s or L/s);
q	unit flow rate (m^2/s);
R^2	coefficient of determination;
S_i	slope of inlet key;
S_o	slope of outlet key;
T_s	weir wall thickness (m);

t	time (min);
t_e	time to equilibrium (min);
U_j	Jet velocity (m/s);
V	average flow velocity (m/s);
W_i	PK weir inlet key width (m);
W_o	PK weir outlet key width (m);
W_u	PK weir cycle width (m);
X_{max}	maximum scour depth location in the along x-axis (m);
X_{pre}	predicted maximum scour depth location in the along x-axis (m);
x	non-dimensional multiple;
Z	scour depth (m);
Z_{apron}	predicted maximum scour depth downstream of an apron (m);
Z_{max}	maximum scour depth (m);
Z_{pre}	predicted maximum scour depth (m);
Z_s	scour depth at a particular point (m);
ρ	density of substrate material (kg/m^3);
σ	non-uniformity coefficient;
γ	specific weight of substrate material (N/m^3);
θ	jet angle;
ϕ	angle of repose of substrate; and
π	pi constant.

INTRODUCTION

Aging hydraulic infrastructure (>50 years old) has increasing risk of increased maintenance, incidents, or failure due to increasing climate variability, flooding, deterioration, not meeting current design criteria, and population growth (Green 2010, Marsooli et al. 2019). Aging structures with poor hydraulic efficiency can increase associated threats and damage due to flooding, which can possibly lead to excessive flood damage costs, affect thousands of individuals, and potentially cause loss of life (FloodList 2020, NWS and NOAA 2020).

Non-linear weirs such as labyrinth and Piano Key (PK) weirs can provide aging infrastructure with increased flow capacity, hydraulic efficiency, a passive flow control (no gates or machinery), and the ability to pass woody debris during flooding episodes (Machiels et al. 2014, López-Soto et al. 2016, Crookston et al. 2019). Labyrinth and piano key (PK) weirs are viable options for in-river rehabilitation projects, but like any other structure, these structures are susceptible to local scour under extreme hydraulic conditions that occur during flooding episodes. Scour is dependent upon various factors namely sediment properties, discharge, duration, tailwater depth, and flow turbulence.

Local scour occurs as energy from the flow is transferred to the bed causing channel degradation (Hoffmans and Verheij 1997, Bombardelli et al. 2018). The scour phenomenon occurs as jets produced by the structure impinge on the adjacent bed material. Jets can be classified due to different characteristics such as orientation, shape (2D or 3D flow field), and whether the jet is plunging or submerged (Mason and Arumugam 1985, Hoffmans and Verheij 1997, Adduce and Sciortino 2006, Dey and Raikar 2007, Pagliara et al. 2008, Bombardelli et al. 2018, Palermo et al. 2018, Meftah

and Mossa 2020). Jets produced by structures require a form of scour mitigation to limit, control, or force scour to occur farther downstream, which will reduce the risk of failure. This mitigation can take the form of aprons, stilling basins, or armoring techniques at the toe of the structure (Novark et al. 1995, Hoffmans and Verheij 1997, Khatsuria 2005, Pfister et al. 2017).

Jets produced by various structures have been studied extensively, but until recently little is known regarding local scour at PK weirs (Jüstrich et al. 2016, Lantz et al. 2020, Pfister et al. 2017). Jüstrich et al. (2016) was the first to produce scour geometry prediction equations for a Type A (Pralong et al. 2011) rectangular PK of weir height, P = 0.15 m. Palermo et al. (2020) studied scour morphology at equilibrium for PK weirs with a P = 0.17 m. Yazdi et al. (2021) studied scour at various rectangular and triangular PK weirs with P = 0.15 m and 0.20 m, produced other prediction equations, and determined that triangular PK weirs produce less scour. Each of these studies were performed with no scour mitigation.

Even with the recent interest in scour at PK weirs, there is little structures-specific design guidance for scour mitigation at PK weirs. The only literature available for scour mitigation at PK weirs is by Pfister et al. (2017). Pfister et al. (2017) outlines the design for a rip-rap plunge pool that can be designed based on scour equations from Jüstrich et al. (2016). The rip-rap plunge pool follows similar contours to the scour hole produced without any mitigation. There is no design guidance for cutoff walls downstream of aprons at PK weirs. Often, engineers design cutoff walls using maximum scour equations, adding factors of safety, and/or keying cutoff walls into competent bedrock.

Due to the lack of information related to scour geometry features, such as maximum scour depth (Z_{max}) and length (L_{max}), and the lack of design guidance for aprons and cutoff walls for PK weirs, a large-scale physical model study is performed at Utah State University. This study will investigate local scour processes downstream of PK weirs by quantifying local scour at the base of a Type A (Pralong et al. 2011) PK weir with and without various size apron mitigation. This study examines scour in two non-cohesive substrates as a function of discharge and tailwater depth. Additionally, this study includes equations that practitioners and researchers can use as references for estimating scour downstream of PK weirs. Lastly, three different size apron lengths are tested to determine adequate scour mitigation for PK weirs. The apron tests are used to create equations to estimate apron length and cutoff wall depth.

EXPERIMENTAL SETUP

This laboratory study involved the design and construction of the experimental flume, fabrication and installation of a PK weir, and the placement and removal of two different substrate materials. For each substrate material, three different apron lengths were installed as scour mitigation. This section will discuss testing facilities, instrumentation, and methodology used for data collection.

Testing Facilities

The physical modeling of the PK weir tested in this study was performed at the Utah Water Research Laboratory (UWRL) at Utah State University in Logan, UT (https://uwrl.usu.edu/) in a newly constructed steel flume (2 m x 16 m x 1.8 m deep) as shown in Fig. 1. The weir was placed on a steel platform 1.09 m above the channel invert, placed 2 m downstream from the rock baffle, and leveled to ±1.6 mm. A scour box was designed (2 m x 5 m x 1.09 m deep) to encase the substrate and allow for a planar bed to be raked uniform to the downstream base of the weir. A clear acrylic sidewall section allowed for scour observations during the duration of an experimental run. To control tailwater depth, a stop log assembly was installed at the far end of the flume and wood strips were added or removed to raise and lower the tailwater level, respectively.

Water was supplied via gravity to the flume through a 30.5 cm (12 in.) or 61 cm (24 in.) diameter pipeline hydraulically connected to a reservoir adjacent to the laboratory. The flow entered the flume via the headbox and was dispersed by a diffuser pipe. The energy of the water was further dissipated by a rock baffle wall, to improve approach flow uniformity.

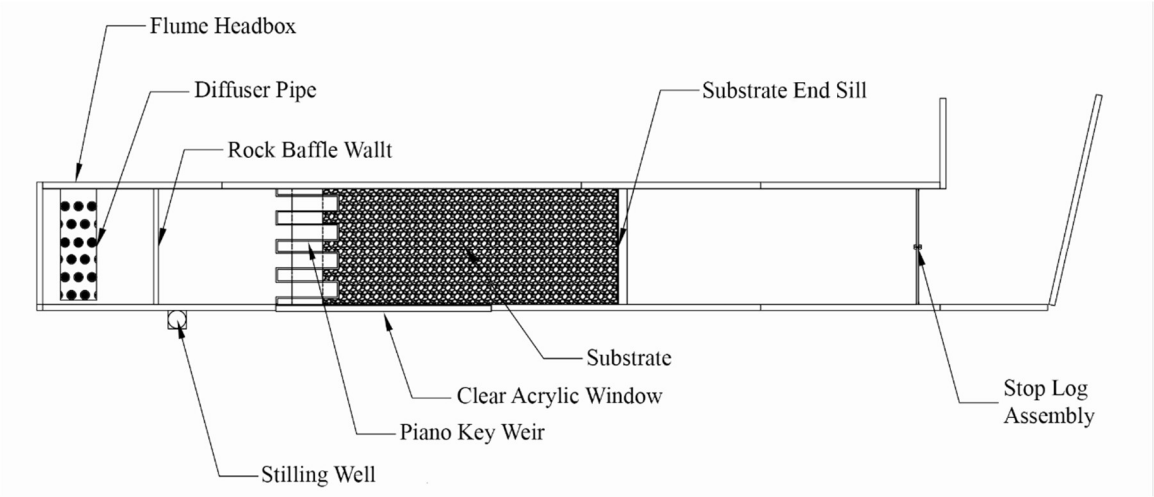

Fig. 1. Plan view of flume, baffle wall, stilling well tap, weir, scour box, and stop log assembly.

Fig. 2. Photograph of the flume in the UWRL.

Physical Model

In this study, only one size and type of PK weir was tested with two different sizes of substrate material. The study was broken into two parts. For part one, each substrate material was tested with three different flow rates and three different tailwater conditions. For part two, each substrate size was tested with three different apron lengths, the same three flow rates, and one tailwater depth. Hydraulic and geometric parameters are presented in Fig. 3 and Fig. 4.

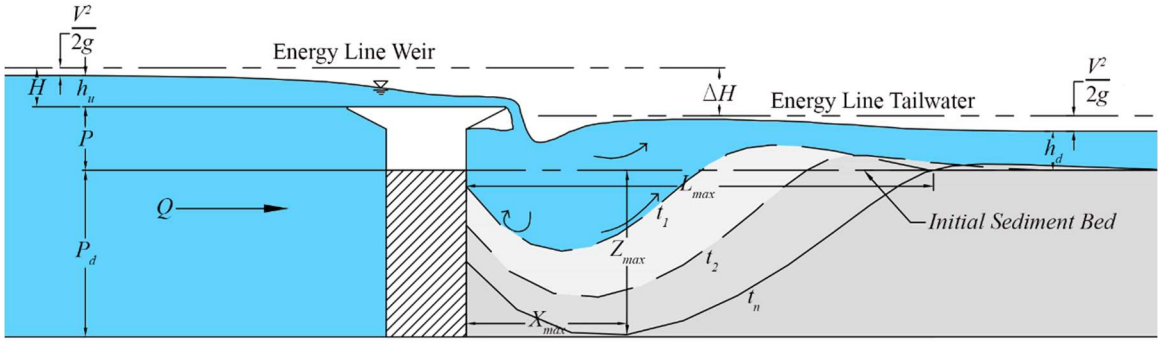

Fig. 3. Hydraulic schematic for the study.

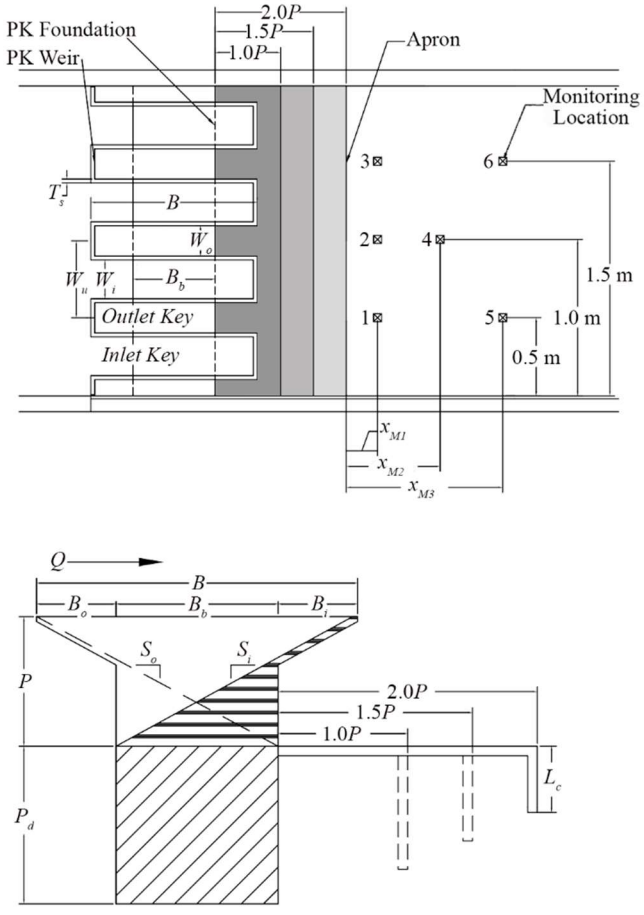

Fig. 4. Geometric schematic of PK weir and apron setup.

The PK weir was constructed using clear acrylic sheeting with P = 42 cm and a nominal wall thickness (T_s), of 2.54 cm. The PK weir is a Type A (Pralong et al. 2011) configuration with four cycles (N = 4), an inlet and outlet key ratio (W_i/W_o) of 1.28, and a flat crest, as shown in Fig. 4. Other PK weir dimensions are summarized in Table 1, where B = streamwise length of the PK weir, B_b = the base length of the PK, B_i = the length of the inlet key, B_o = the length of the outlet key, S_o = slope of the outlet key, S_i = slope of the inlet key, W_u = cycle width, W_i = width of the inlet key, W_o = width of the outlet key, and P_d = height of the PK weir base. The aprons and cutoff walls used in the study were constructed using painted plywood sheeting and anchored using lumber and sediment weight. Specific aprons lengths used in the study were 1.0P (42 cm), 1.5P (63 cm), and 2.0P (0.84 m). The cutoff walls were constructed to a conservative depth based on preliminary scour testing to ensure no scour undermining of the structure.

Table 1– PK weir parameters.

Parameter	**Value**
B	1.04 m
B_b	0.52 m
Bi=Bo	0.26 m
S_o=S_i	0.55
W_u	0.49 m
N	4.00
P	0.42 m
T_s	.025 m
W_i/W_o	1.28
Crest Type	Flat
P_d	1.09 m

The study used two non-cohesive substrate materials of varying sizes. To differentiate between the substrate materials, substrate material number 1was referred to as the coarse substrate and substrate material number 2 was referred to as the fine

substrate material. Granulometric properties for each of the substrate materials is summarized in Table 2 where d_{90} = diameter where 90% of substrate material is finer, d_{50} = median substrate size, coefficient of gradation $\sigma = (d_{84}/d_{16})^{1/2}$, ρ = density, γ = specific weight, and G = specific gravity. The sieve analysis conducted for the two different substrate materials is shown in Fig. 5. Both substrate materials were considered uniform, or of an even particle distribution. A side by side comparison of the substrate material is given in Fig. 6.

Table 2 – Substrate granulometric properties.

	Substrate 1	**Substrate 2**
d_{90} (mm)	20.00	9.10
d_{50} (mm)	13.00	6.50
σ	1.54	1.30
ρ (kg/m^3)	2,604.28	2,646.89
γ (N/m^3)	25,547.98	25,965.99
G	2.61	2.65

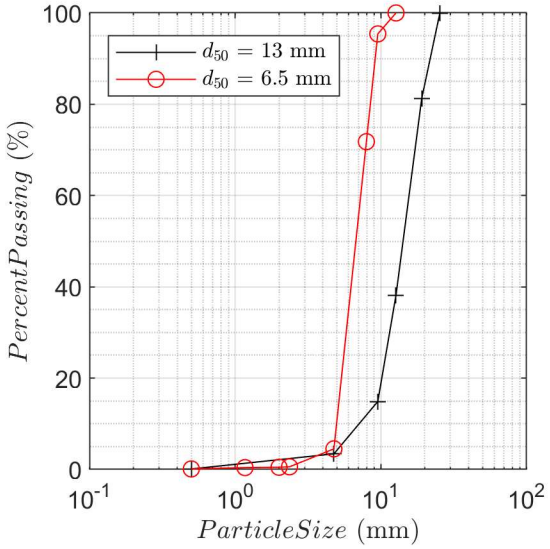

Fig. 5. Sieve analysis for the two-substrate material.

Fig. 6. Substrate material comparisons.

Instrumentation

The water supply lines (30.5- and 61-cm diameter pipes) were routed through a calibrated venturi flow meter with an average uncertainty of ±0.25% (see Fig. 7). To measure the flow through the supply lines, a pressure transducer was attached to the venturi meter's pressure taps. A multimeter was attached to the pressure transducer, and the pressure transducer's range and zero were set using a Hart communicator sensor. The output frequency from the multimeter was displayed in mA, and the multimeter output was recorded and converted to a pressure differential. The corresponding discharge was determined using flow meter calibration data. For one data point, a continuous running average was taken and checked every three to five minutes from the beginning of an experimental run to ensure that steady-state conditions were achieved. As the experiment continued, the flowrate was checked every thirty minutes to an hour to ensure continuous steady-state conditions.

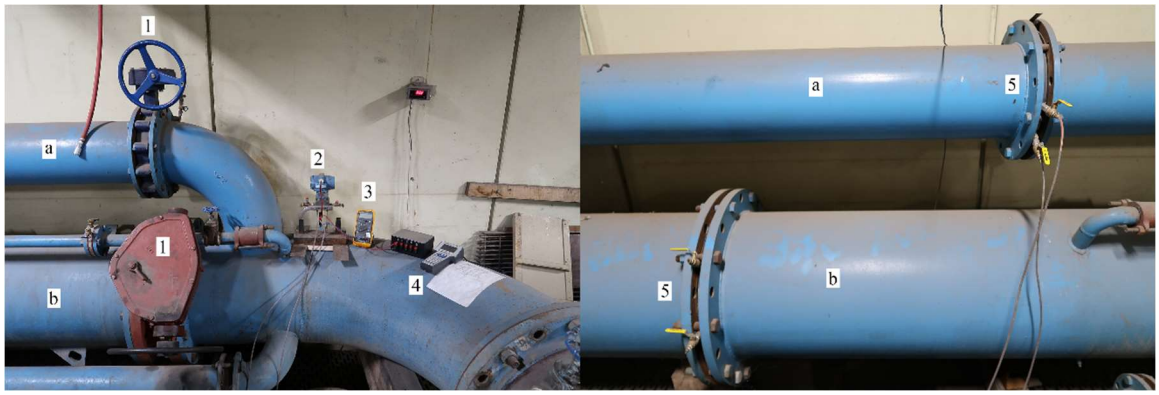

Fig. 7. 30.5 cm (a) and 61 cm (b) diameter supply lines with butterfly control valves (1), pressure transducer (2), multimeter (3), Hart communicator sensor (4), and Venturi meter pressure taps (5).

To measure the constantly fluctuating and dynamic water surface in the flume, a stilling well was hydraulically connected to the side of the flume two meters upstream of the weir and equipped with a calibrated, precision point gauge (accurate within ±0.152 mm). The stilling well measured the piezometric head upstream of the weir. Downstream of the weir, an ultrasonic sensor (Microsonic mic+130/IU/TC) was used to measure the fluctuating water surface elevation. The ultrasonic sensor was accurate to ±1% when the sensor's internal temperatures reached optimal operating temperature, after approximately 30 minutes (Microsonic 2020). Measuring the dynamic downstream water depth allowed researchers to determine the effects of tailwater depth on scour morphology.

To monitor the morphology throughout the run, columns of spheres were buried in the substrate material (Fig. 4). The streamwise station (x_{mi}) for the sphere installations varied with downstream apron details and substrate type. Depending on the substrate material and corresponding nature of the scour hole geometry, the sphere's location x_{mi} was changed to capture the morphology of the substrate material. The locations of x_{mi} are

summarized in Table 3. To ensure the release of the spheres coincided with exposure due to scour, the buoyancy of the spheres was reduced to slightly positive by injecting 15 ml of silicon into each sphere (G = 0.53). This allowed the sphere to stay in place until the top half of the sphere was uncovered, which produced a ±1.25 cm accuracy in estimating scour depth (Fig. 8). Once the spheres surfaced, a video array setup to capture the spheres would record their appearance for later review.

Table 3 – x_{mi} location based on substrate material.

	Substrate 1	**Substrate 2**
x_{m1}	0.2 m	0.5 m
x_{m2}	0.6 m	1.0 m
x_{m3}	1.0 m	1.5 m

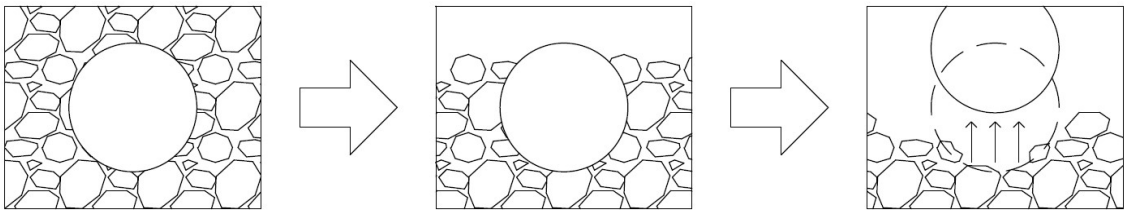

Fig. 8. Sphere animation as scour occurs.

To document geometric scour features of the substrate bed, a RealSense D435 depth camera was used to scan the bed following the completion of each test. The D435 camera features, summarized in Table 4, show the camera is accurate to ±1 mm when used within a camera to object range of 0.6 m and 0.8 m. A customized, USU MATLAB script was developed to process camera images to estimate scour features. These features were checked after each experimental run by taking hand measurements using a

retractable measuring device, which was attached to a moving cart on the flume. The retractable measuring device was accurate to within ±1 mm.

Table 4 – Intel RealSense D435 depth camera features.

Feature	**Detail**
Global Shutter	3µm × 3µm pixel size
IR Stereo: FOV	86°×57° (±3°)
IR Stereo: Resolution	1280×720
RGB: FOV	64°×41°×77° (±3°)
RGB: Resolution	1920×1080

METHODOLOGY

The study was separated into two parts. Part one focuses on scour formation without an apron. Part two focuses on the change of scour formation with the addition of an apron. For each part of the study, both substrates are used in the experiment, but each part had varying hydraulic conditions.

Piano Key Weir Geometric Effects on Scour Morphology

To determine the effects that a Type A (Pralong et al. 2011) PK weir had on scour, the same hydraulic conditions were tested with each substrate material. The hydraulic conditions that were considered for each substrate material are shown in Table 5. Each substrate material was scoured to a steady-state condition for three different flow rates and three different tailwater conditions.

Table 5 – Test matrix for the PK weir geometric effects on scour morphology study.

Substrate Type	Discharge	Headwater	Tailwater
d_{50} = 6.5 mm d_{50} = 13 mm	150 l/s	$H/P \approx 0.11$	$0.3P \approx 14$ cm
			$0.6P \approx 28$ cm
			$1.0P \approx 42$ cm
	300 l/s	$H/P \approx 0.18$	$0.3P \approx 14$ cm
			$0.6P \approx 28$ cm
			$1.0P \approx 42$ cm
	600 l/s	$H/P \approx 0.35$	$0.3P \approx 14$ cm
			$0.6P \approx 28$ cm
			$1.0P \approx 42$ cm

To begin each experiment and to minimize local velocities and shear stresses on the substrate, the flume was slowly filled until a weir-submerging tailwater depth was achieved. Once the target discharge was set, the tailwater was lowered to the target value, the timer and video camera array were started, and the test began. Throughout the

duration of the run, scour observations were taken periodically to monitor scour evolution. At the beginning of the run, observations were taken every half minute to minute until the high rate of scour decreased, which typically lasted 30 minutes.

To determine when the experiment had reached a quasi-equilibrium state, a selection of tests were repeated and performed for over 18 hrs to ensure that the maximum scour was achieved. The repeated tests were monitored until the percent difference in total scour depth and length was within a 5% threshold of the maximum scour depth and length. The threshold time determined the desired duration for each experimental run. The run-duration varied depending on flow rate and tailwater conditions. No experimental run, other than those with no observed scour, ran less than three hours.

Apron and Cutoff Wall Design Study

To determine the change in geometric scour features due to the addition of mitigation, three different aprons were tested with the coarse and fine substrate materials. The aprons were tested to determine how various apron lengths mitigated and moved the geometric scour features downstream of the PK weirs. The hydraulic conditions associated with experimental runs involving the aprons are shown in Table 6.

Table 6 – Test matrix for the apron and cutoff wall design study.

Substrate Type	Discharge	Headwater	Tailwater	Apron Length
d_{50} = 6.5 mm d_{50} = 13 mm	150 l/s	$H/P \approx 0.11$	$0.3P \approx 14$ cm	$2.0P = 0.84$ m
				$1.5P = 0.63$ m
				$1.0P = 0.42$ m
	300 l/s	$H/P \approx 0.18$	$0.3P \approx 14$ cm	$2.0P = 0.84$ m
				$1.5P = 0.63$ m
				$1.0P = 0.42$ m
	600 l/s	$H/P \approx 0.35$	$0.3P \approx 14$ cm	$2.0P = 0.84$ m
				$1.5P = 0.63$ m
				$1.0P = 0.42$ m

EVOLUTION OF LOCAL SCOUR DOWNSTREAM OF A TYPE A PK WEIR IN NON-COHESIVE SEDIMENTS

Abstract

Increased frequency and severity of flooding events due to climate change and other factors have resulted in scour damage to various hydraulic structures and motivated rehabilitation projects. Non-linear weirs, such as labyrinth and piano key weirs, are often considered for rehabilitation projects due to their passive flow control nature, hydraulic efficiency, and construction economy. A large-scale piano key weir laboratory study is performed to investigate susceptibility to downstream scour of two non-cohesive substrate materials. Results include scour evolution, scour hole geometry, and scour patterns. Hydraulics conditions, particularly tailwater conditions, can significantly impact the amount, evolution, and final morphology of local scour. Results found that for high flow and low tailwater conditions maximum scour depths greatly exceeded the weir height. The results of this study can inform the estimation of maximum scour depth, maximum scour position in the streamwise direction, and maximum scour length that may occur.

Keywords: local scour, piano key weir, temporal evolution, equilibrium, non-cohesive sediment

Introduction

Flooding incidents around the world are occurring with greater frequency and magnitude, resulting in increased impacts on many urban communities. It is estimated that the 100-year return period floods are occurring at three times the frequency of

historical records (Marsooli et al. 2019). For example, three significant flooding events occurred in 2019 (FloodList 2020) along the Missouri and Mississippi rivers in the U.S with billions of dollars in damage and millions of people directly affected (Center for Disaster Philanthropy 2019, NWS and NOAA 2020). Due to flooding consequences, climate change, and population growth, the need for sustainable flood risk management is increasing (Green 2010).

Flow control structures commonly used in channels and for flood protection schemes include dams and levees, spillways, and various types of gates and weirs. Some aging structures (>50 years old) that do not meet current hydraulic design criteria and/or have other safety deficiencies are being rehabilitated; labyrinth or piano key weirs (PK weirs) are regularly considered due to improved hydraulic efficiency, compact footprint, techno-economic viability, and passive flow control nature (Machiels et al. 2014, López-Soto et al. 2016, Crookston et al. 2019). However, local scour mitigation at weirs and other drop structures remains a challenging task in design as scour evolution is highly dependent upon local geological and hydrological conditions, hydraulic structure geometry, and the complexities of water interacting with sediments and rock (Hoffmans and Verheij 1997, Ettema et al. 2004, Bombardelli et al. 2018, Lantz et al. 2020, Meftah and Mossa 2020).

Scour at the downstream base of weir-like structures such as labyrinth and PK weirs, ogee weirs, broad-crested weirs, rock weirs, and similar grade control structures is considered jet-induced scour (Aderibigbe and Rajaratnam 1998), which can be classified as two major types: 1) plunging jets or 2) submerged jets (Hoffmans and Verheij 1997, Jia et al. 2001). Plunging jet scour has been extensively researched for a variety of

hydraulic structures with three major subgroups: cylindrical jets, angled ramp jets ranging from vertical to horizontal, and free fall jets (e.g., Mason and Arumugam 1985, Adduce and Sciortino 2006, Dey and Raikar 2007, Pagliara et al. 2008, Bombardelli et al. 2018, Palermo et al. 2018). Additionally, the temporal evolution of scour and maximum scour depth predictions for these different subgroups provide guidance for practitioners to estimate scour evolution and formulate mitigation or scour protection measures (Schoklitsch 1932, Mason and Arumugam 1985, Bormann and Julien 1991, Kuhnle et al. 2002, Nasrollahi et al. 2008, Chen et al. 2016, Wang et al. 2019, Meftah and Mossa 2020).

It is evident in published literature that the geometry of the hydraulic structure in combination with hydraulic conditions directly influences scour features, which include maximum scour depth (Z_{max}), maximum scour depth location in the streamwise direction (X_{max}), scour hole length (L_{max}) and other local scour patterns. Therefore, laboratory studies and field observations specific to PK weirs are needed to make structure-specific scour evaluations (Jüstrich et al. 2016, Pfister et al. 2017, Lantz et al. 2020).

Currently, limited research is published on local scour at non-linear weirs. Upstream siltation and sediment removal for PK and labyrinth weirs were investigated by Gebhardt et al. (2019) and Noseda et al. (2019). Gebhardt et al. (2019) concluded that the shape of the labyrinth weir produces a horseshoe-vortex in the inlet key causing sediment transport. Noseda et al. (2019) concluded that scour upstream of the weir can exceed the weir height (P). Elnikhely and Fathy (2020) created a prediction method for scour at various apex angles for triangular labyrinth weirs with a downstream apron. Elnikhely and Fathy (2020) concluded that in comparison to linear weirs, labyrinth weirs produce

less scour and labyrinth weirs with side wall angles of 60° produced the least amount of scour downstream of the apron. Yazdi et al. (2021) studied scour downstream of both rectangular and triangular PK weir geometries with P = 0.15 m and 0.20 m for a non-cohesive gravel with a median gravel size, d_{50} = 7.8 mm. Yazdi et al. (2021) created prediction methods to estimate Z_{max}, X_{max} and L_{max} for both weir geometries, and determined that triangular PK weirs produce less scour on average than rectangular PK weirs. Palermo et al. (2020) evaluated equilibrium morphology at PK weirs and analyzed the scour mechanisms that produce bed formations downstream. Jüstrich et al. (2016) and companion study Pfister et al. (2017) studied riverbed scour at PK weirs and produced scour prediction methods that determine Z_{max}, X_{max}, and L_{max}. Jüstrich et al. (2016) evaluated multiple other scour prediction methods specific to other structures for comparison. Pfister et al. (2017) focused on scour mitigation at PK weirs using rip-rap protection using the maximum scour geometries predicted by Jüstrich et al. (2016). However, additional information and insight on the scour evolution at the toe of a PK weir is needed.

Therefore, a large-scale (P=0.42 m) (88% of all constructed PK weirs have 1 m ≤ P ≤ 6 m) physical model study is performed with a Type A (Pralong et al. 2011) PK weir geometry and two non-cohesive substrate materials for a range of hydraulic conditions (Crookston et al. 2019). Results include jet characteristics generated by the PK weir, resulting maximum scour features developed as a function of time, and information to inform scour prediction in the field.

Experimental Setup

Facility

This study was conducted at the Utah Water Research Laboratory at Utah State University in a rectangular flume (2-meter wide, 1.8-meter deep, and 16-meter long) (see Fig. 9). The headbox for the flume featured a diffuser and rock baffle to provide uniform tranquil flows to the PK weir. Tailwater (h_d) was controlled with a downstream stop log assembly. The mobile bed section of the flume was 1.09 m deep and featured a clear acrylic sidewall panel for monitoring and documentation. The PK weir geometry is summarized in Fig. 10 and Table 7 where B = streamwise length of the PK weir, B_b = streamwise length of the base of the PK, B_i = the length of the inlet key, B_o = the length of the outlet key, S_o = slope of the outlet key, S_i = slope of the inlet key, W_u = cycle width, N = number of cycles, P = weir height, T_s = sidewall thickness, W_i = inlet key, W_o = outlet key, and P_d = PK weir base. Monitoring locations in the streamwise direction (x_{mi}) varied based on the substrate material (Table 3).

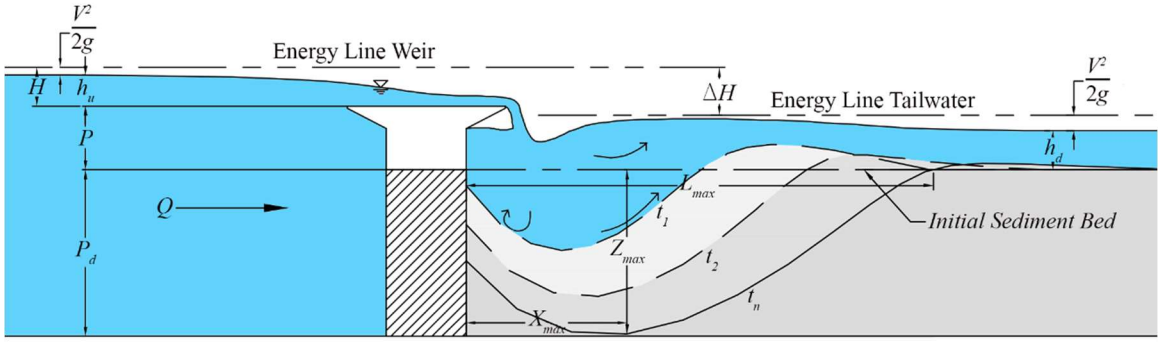

Fig. 9. Illustration of experimental setup with PK geometry and scour morphology.

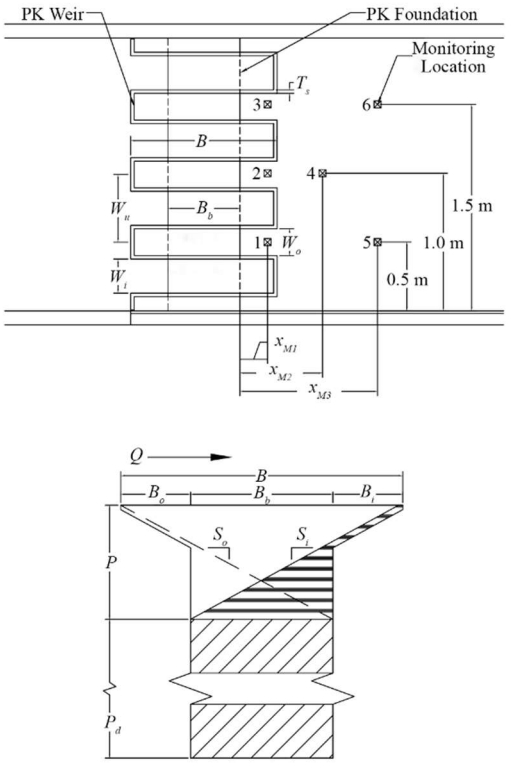

Fig. 10. Geometric and hydraulic parameters of this study.

Table 7 – Geometric parameters of the PK weir.

Parameter	Value
B	1.04 m
B_b	0.52 m
B_i=B_o	0.26 m
S_o=S_i	0.55
W_u	0.49 m
N	4.00
P	0.42 m
T_s	0.025 m
W_i/W_o	1.28
Crest Type	Flat
P_d	1.09 m

Substrate

The study was performed with two types of substrate. To differentiate between the two substrate materials, substrate material 1 was referred to as the coarse substrate and substrate material 2 was referred to as the fine substrate (Table 8). Both substrate types were angular, relatively uniform (Fig. 11) non-cohesive gravels, with varied granulometric properties (Table 8) where d_{90} = diameter where 90% of material is finer, d_{50} = median gravel size, coefficient of gradation $\sigma = (d_{84}/d_{16})^{1/2}$, ρ = substrate density, γ = substrate specific weight, and G = substrate specific gravity. Uniformly graded substrates were defined as a gradation consisting of particles of similar size. The results of this study are limited to the materials tested; however, Annandale (1995) and the Erodibility Index Method could be considered to scale the results to other material sizes.

For each laboratory test, the gravel substrate material was prepared by uniformly adding gravel and raking until a planar bed was achieved that was level with the base of the PK weir. No additional compaction of the material was performed, so as to mimic natural river deposits. Material deposited downstream of the scour hole during a test was not manually removed, thus any bedforms were allowed to form and evolve and the results were more representative of field conditions where river sediments would be deposited adjacent to the scour hole, not transported farther downstream.

Table 8 – Granulometric properties of the substrate materials.

	Substrate 1	**Substrate 2**
d_{90} (mm)	20.00	9.10
d_{50} (mm)	13.00	6.50
σ	1.54	1.30
ρ (kg/m^3)	2,604.28	2,646.89
γ (N/m^3)	25,547.98	25,965.99
G	2.61	2.65

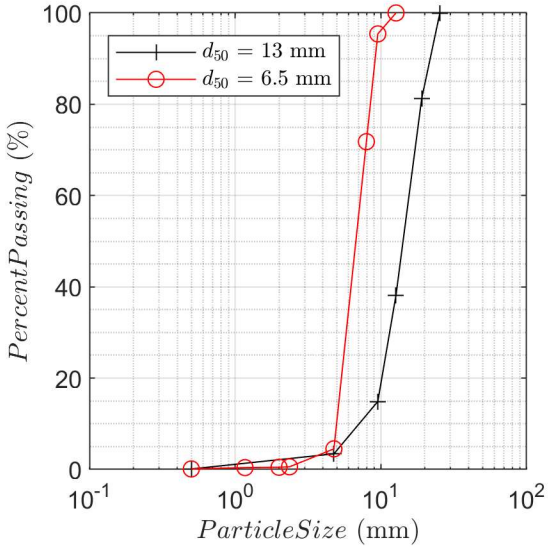

Fig. 11. Sieve analysis for substrate material.

Instrumentation

A calibrated venturi meter (±0.25%) was used to measure discharge supplied to the PK weir and movable bed. Headwater elevations were measured two meters upstream of the weir with a stilling well and point gage (±1.5 mm). Ultrasonic sensors (Microsonic mic+130/IU/TC) were used to measure the dynamic headwater (h_u) and tailwater (h_d) surface at two locations within the flume (± 1% accuracy) (Zhang et al. 2018, Microsonic 2021). Measuring the water surface elevation determined the tailwater depth, and corroborated the stilling well headwater depth.

Scour morphology was measured using two techniques. First, the gridded observation window was used with video recordings and photos to document temporal scour hole development; however, this method only documented particle movement immediately adjacent to the window. A second technique employed small, slightly positively buoyant, spheres (G = 0.53) forming vertical columns buried in the substrate

near the flume centerline (Fig. 10). As scour evolved and material was removed, a buoyant sphere would gradually become exposed. At about 50% exposure (Fig. 12), the sphere would escape and rise to the surface, providing a temporal record of scour depth by location. Sphere locations were color coded by columns, and spheres surfacing were documented with video recordings. To avoid premature removal of the spheres prior to exposure, the specific gravity of the spheres was controlled by filling each sphere with 15 ml of silicone.

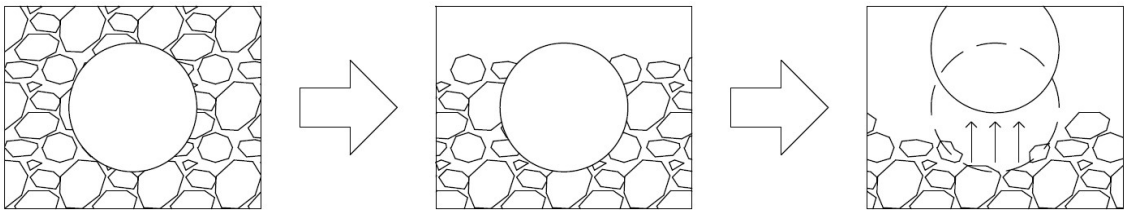

Fig. 12. Controlled specific weight of spheres minimize premature evacuation from substrate.

To quantify the post-scour morphology or maximum scour geometry at equilibrium, an Intel-RealSense stereo imaging camera was used to scan the downstream bed topography (Bung et al. 2020) (±1.0 mm accuracy operated within 0.6 m and 0.8 m range). Each camera scan was verified by taking vertical point measurements on a grid with a point gage (±1 mm) mounted to a flume carriage. The camera was operated with a global shutter and 3μm × 3μm pixel size. The depth properties included active IR stereo, field of view (FOV) 86°×57° (±3°), a max output resolution of 1280×720. The RGB camera properties included a rolling shutter, a max resolution of 1920×1080, an FOV of 64°×41°×77° (±3°). A MATLAB script was developed to post-process the scanned images into a single image and gather various scour dimensions. The script also

generated various plots of 2D and 3D scour profiles to communicate maximum scour features.

Testing Scheme

The test matrix for this study is presented in Table 9, which notes flow rate (*Q)* and corresponding h_d elevations for each experimental test. The target h_d included 0.33*P*, 0.66*P*, and 1.0*P*. Repeatability was included for four tests (Table 10). The minimum achievable h_d varied with *Q*. Tailwater measurements were taken 4.75 m downstream of the weir. Substrate deposition occurred upstream of the h_d measurement point and had no effect on the h_d measurements.

Table 9 – Test matrix for study.

Substrate Properties	**Discharge, *Q***	**Headwater Ratio, *H/P***	**Tailwater Depth, h_d**
Coarse Gravel: d_{90} = 20 mm, d_{50} = 13 mm, σ = 1.54, G = 2.61 Fine Gravel: d_{90} = 9.1 mm, d_{50} = 6.5 mm, σ = 1.30, G = 2.65	150 L/s	0.11	Actual = 0.38*P*
			Actual = 0.62*P*
			Actual = 1.0*P* cm
	300 L/s	0.18	Actual = 0.40*P*
			Actual = 0.59*P*
			Actual = 1.02*P*
	600 L/s	0.35	Actual = 0.52*P*
			Actual = 0.66*P*
			Actual = 1.02*P*

Testing Methodology

To begin each experiment and to minimize any pre-scour (i.e., local velocities and shear stresses on the substrate), the flume was slowly filled until the weir was submerged. The target Q was then set, the h_d or minimum permissible h_d was set, and upon setting the h_d the timer and video recordings were initialized. Throughout the duration of each test, scour observations were taken regularly via the observation window and grid to monitor scour evolution. At the beginning of each test, observation frequency was high (results recorded every 30-60 s) until the rate of scour reduced or observed values became redundant, at which point less frequent observations were permissible (typically after the initial 30 minutes of each experiment). Test durations were carefully checked to confirm equilibrium by monitoring Z_{max}, X_{max}, and L_{max}, etc., with the highest Q and lowest h_d combinations lasting 18 hrs or longer. Minimum required test durations for lowest Q and highest h_d were shorter, with equilibrium achieved in under 3 hrs. All tests were concluded after equilibrium was achieved, where equilibrium was defined as less than 5% change in all scour hole geometry parameters (often less than 1%).

Results

Scour-inducing PK Weir Hydraulics

Unique scour patterns were observed downstream of a PK weir due to jets produced by the weir geometry. The majority of the flow was concentrated in the outlet keys and produced a rotating, plunging oblique jet with trajectory matching S_o (see Fig. 13). The weir inlet keys produced a near-vertical discharge plunging jet (see Figs. 13 and 14) that impinged upon the bed material; however, this jet had less energy to scour the

substrate than the oblique jets in part due to the lower local unit discharge. As flows passed over the PK weir, air was entrained across the entire weir width, resulting in localized flow bulking. These PK weir jet hydraulic conditions were modified when the jets became submerged or as the h_d approached 1.0P, which caused less erosion to occur.

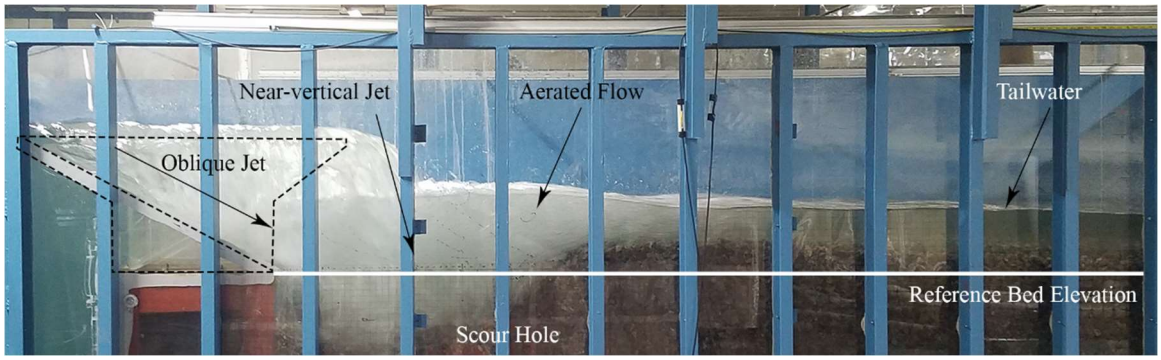

Fig. 13. Three-dimensional jet patterns produced by PK weir.

Fig. 14. Channel view of PK weir.

Temporal Evolution

The PK weir impinging jets produced a local scour hole that increased in depth and length with time until reaching equilibrium. Scour hole evolution was observed to occur during three main phases (Fig. 15A). During the initial phase, shear stresses on the material significantly exceeded the critical shear stress causing many particles to be

transported as bedload (sliding and saltating) for the $d_{100} - d_5$ gravel size fractions with the remainder moving as suspended load. Scour in the vertical direction was more rapid than in the streamwise direction during this phase, influenced by the oblique jet angle. As local velocities reduced in the streamwise direction material was often deposited immediately downstream of the scour hole, causing the formation of a dune. For the lowest h_d and highest Q combinations, material was transported beyond the substrate bed section of the flume.

Fig. 15A-C. Scour development with time for (A) Initial Phase, (B) Second Phase, and (C) Final Phase (timer displays time of observation).

After the initial PK weir scour phase, the scour hole evolved primarily in the streamwise direction and scour in the vertical direction continued at a slower rate. During this second phase the location of the Z_{max} migrated downstream and the angle of repose was established, resulting in groups of particles sliding from the sides towards the bottom of the scour hole. This process had two additional results: 1) some few particles were pulled towards the base of the PK weir forming a slope, and 2) an armoring effect occurred (Fig. 16A and B).

The overall scour evolution and scour hole geometry was not uniform across the width of the PK weir. Due to the PK geometry and corresponding impinging jets, a

trough and ridge pattern formed across the flume. These features aligned with the PK weir keys.

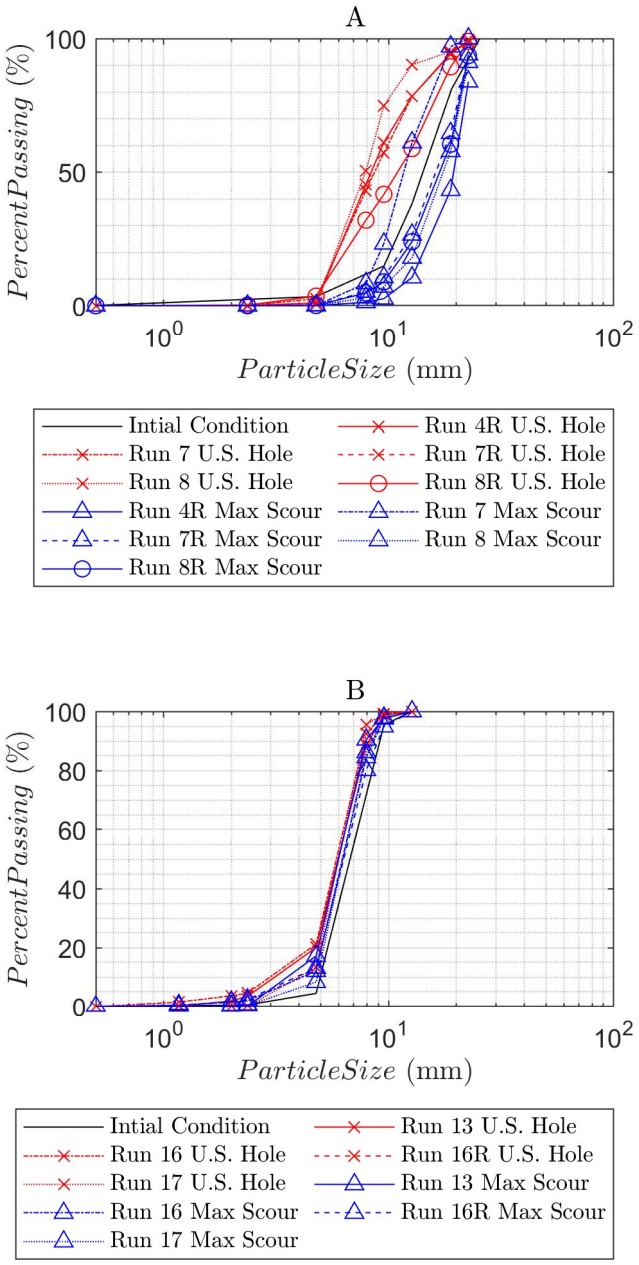

Fig. 16A and B. Sieve analysis of the bed material from the upstream slope of the scour hole and the max scour location, where (A) represents coarse substrate and (B) fine substrate material.

The final and third phase of PK weir scour evolution was characterized by no significant horizontal or vertical scour (see Fig. 15C) (Hoffmans and Verheij 1997). More armoring of the scour hole was observed during this phase, with the smallest particles either transported beyond the movable bed or deposited immediately downstream of the scour hole.

Graphical Prediction of PK Weir Scour

Due to the steady-state nature of the experiment, practitioners could use the temporal evolution (Fig. 19) and Z_{max} (Figs. 17 and 18) graphs to evaluate hydrographs and potential scour at PK weirs. As shown, the scour evolution and maximum geometry varied due with sediment size (Fig. 17A and B). The fine substrate took approximately t=2-6 hours longer to reach an equilibrium state (Table 10). The fine substrate had an average increase in Z_{max} of about 72% relative to the coarse substrate (Comparison of Fig. 18A and B and Table 4). Additionally, the fine substrate had an average increase in L_{max} of 48% relative to the coarse substrate (Fig. 19B and D and Table 10).

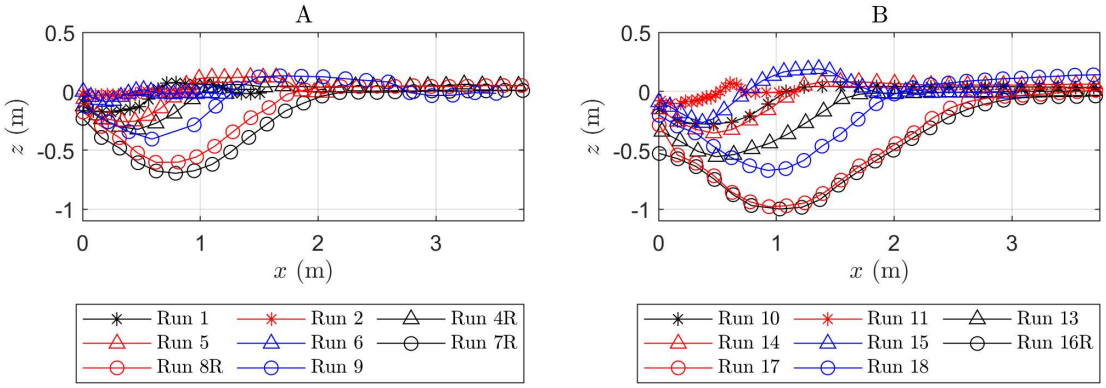

Fig. 17A and B. Maximum scour profiles for (A) coarse substrate and (B) fine substrate material. Table 10 can be used as a reference for hydraulic conditions and scour features.

Table 10 – Maximum scour parameters from each experimental run, where xR specifies a rerun for that experimental run.

Run #	d_{50} (mm)	Time (min)	Q (L/s)	q (m2/s)	h_d (m)	Z_{max} (m)	X_{max} (m)	L_{max} (m)	V (m^3)
1	13.0	180	150	0.08	0.16	-0.18	0.21	0.61	0.12
2	13.0	180	150	0.08	0.26	-0.04	0.07	0.50	0.02
3*	13.0	0	150	0.08	0.42	No Scour			
4	13.0	240	300	0.15	0.21	-0.36	0.48	1.07	0.42
4R	13.0	480	300	0.15	0.17	-0.33	0.42	1.04	0.36
5	13.0	180	300	0.15	0.25	-0.26	0.38	0.82	0.22
6	13.0	180	300	0.15	0.43	-0.09	0.21	0.42	0.03
7	13.0	1200	600	0.30	0.23	-0.83	0.89	2.99	1.98
7R	13.0	900	600	0.30	0.22	-0.71	0.69	2.20	1.49
8	13.0	960	600	0.30	0.28	-0.68	0.71	1.97	1.22
8R	13.0	900	600	0.30	0.29	-0.63	0.70	1.80	1.11
9	13.0	300	600	0.30	0.43	-0.41	0.62	1.28	0.57
10	6.5	450	150	0.08	0.10	-0.28	0.40	1.07	0.39
11	6.5	240	150	0.08	0.27	-0.11	0.16	0.51	0.04
12*	6.5	0	150	0.08	0.43	No Scour			
13	6.5	1050	300	0.15	0.14	-0.56	0.52	1.81	1.03
14	6.5	900	300	0.15	0.25	-0.36	0.49	1.16	0.50
15	6.5	840	300	0.15	0.42	-0.27	0.39	0.74	0.19
16	6.5	1380	600	0.30	0.25	-1.06	0.99	3.35	3.61
16R	6.5	1170	600	0.30	0.22	-1.01	1.00	3.19	3.36
17	6.5	960	600	0.30	0.28	-0.99	1.04	3.43	3.14
18	6.5	1020	600	0.30	0.43	-0.68	0.89	2.04	1.38

*No scour observed

Tailwater depth was a prime factor in scour evolution. For a particular Q, higher h_d led to a decrease in the size of the scour hole and an increase in material deposited as a dune (Fig. 17A and B). This trend can be observed for each Q, namely between experimental Runs 7R and 9 (Fig. 17A) and Runs 13 and 15 (Fig. 17B). The average reduction in scour for high h_d and medium h_d relative to low h_d was 66.6% and 34.5%, respectively (Fig. 18A and B). Scour increases as Q increases. It was determined that the average reduction in scour was 88.1% and 59.4% for Q = 150 and 300 l/s, respectively,

relative to Q = 600 l/s. As Q increases and as h_d decreases no dunes were deposited adjacent to the scour hole for the lowest h_d tested. The only exceptions were for Q = 150 l/s (Fig. 17A and B).

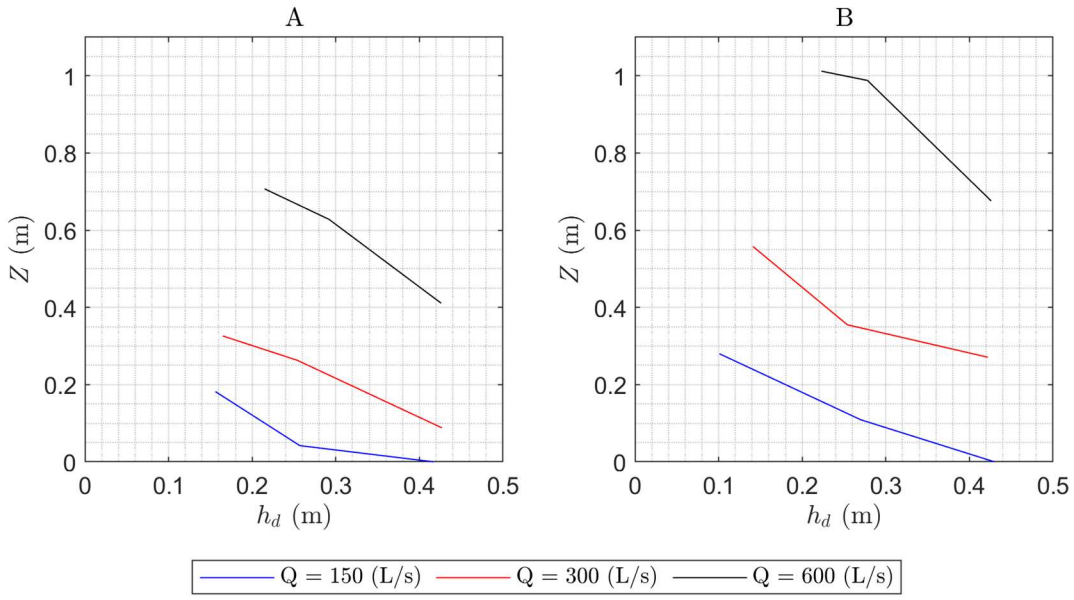

Fig. 18A and B. Tailwater to maximum scour rating curves (A) coarse substrate and (B) fine substrate material.

The Q, h_d condition, and substrate properties affect how long it takes the scour hole to reach equilibrium (Fig. 19A-D). The amount or volume of scour that occurred during Phase 1 increased as Q increased and h_d decreased. It was determined that the majority (>50%) of the maximum scour depth occurred within Phase 1 (Fig. 19A-D). From a design standpoint, the length of the peak of a hydrograph can help to dictate the design of downstream scour mitigation. Increasing Q is proportional to scour, whereas increasing h_d is inversely proportional to scour evolution (Fig 18A and B). As Q increases, scour increases and the time required to reach equilibrium increases. Run 1, Run 4R and Run 7R (Fig 19A and B) and Run 10, Run 13, and Run 16R (Fig. 19C and

D) can be compared to determine how Q affects the time evolution of scour. As h_d increases, scour decreases and equilibrium conditions will occur more rapidly. Run 4R, Run 5, and Run 6 (Fig. 18A and B) and Run 13, Run 14, and Run 15 (Fig. 18C and D) can be compared to determine how h_d affects the time evolution of scour. Lastly, a comparison of Fig. 19A and 19B to Fig. 19C and 19D show how substrate characteristics affect the amount of time it takes for scour to reach equilibrium.

To determine the temporal evolution of scour, a classical method by Nasrollahi et al. (2008) was applied to the results of PK weir scour testing (Fig. 20) (the Nasrollahi et al. (2008) temporal prediction method was developed for scour at spur dikes), as shown in Eq. 1:

$$\frac{Z_{max}}{Z_s} = 1 - \exp\left[-a\left(\frac{t}{t_e}\right)^b\right] \quad (1)$$

where t_e is time to reach equilibrium, t is time at a given point or observation, Z_s is the scour at time t, Z_{max} is scour at equilibrium t_e, and a and b are linear and exponential coefficients. The coefficients are determined experimentally from the study of scour at PK weirs to find a line of best fit for the temporal evolution of scour (see Fig. 19). For the coarse substrate material, the error ranged from 0 – 77% (Fig. 20A). For the fine substrate material, the error ranged from 0 – 44% (Fig. 20B). The error was minimized to find the curve of best fit.

For this study, a = 1.87 and b = 0.18 for coarse substrate (Fig. 20A) and a = 1.95 and b = 0.19 for fine substrate (Fig. 20B). The similarity in coefficients between the two substrate materials shows that substrate material size has minimal impact on the average

temporal evolution of scour at PK weirs. A maximum threshold line was plotted to encompass all runs, which had coefficients $a = 4.42$ and $b = 0.23$ (Fig. 20A and B).

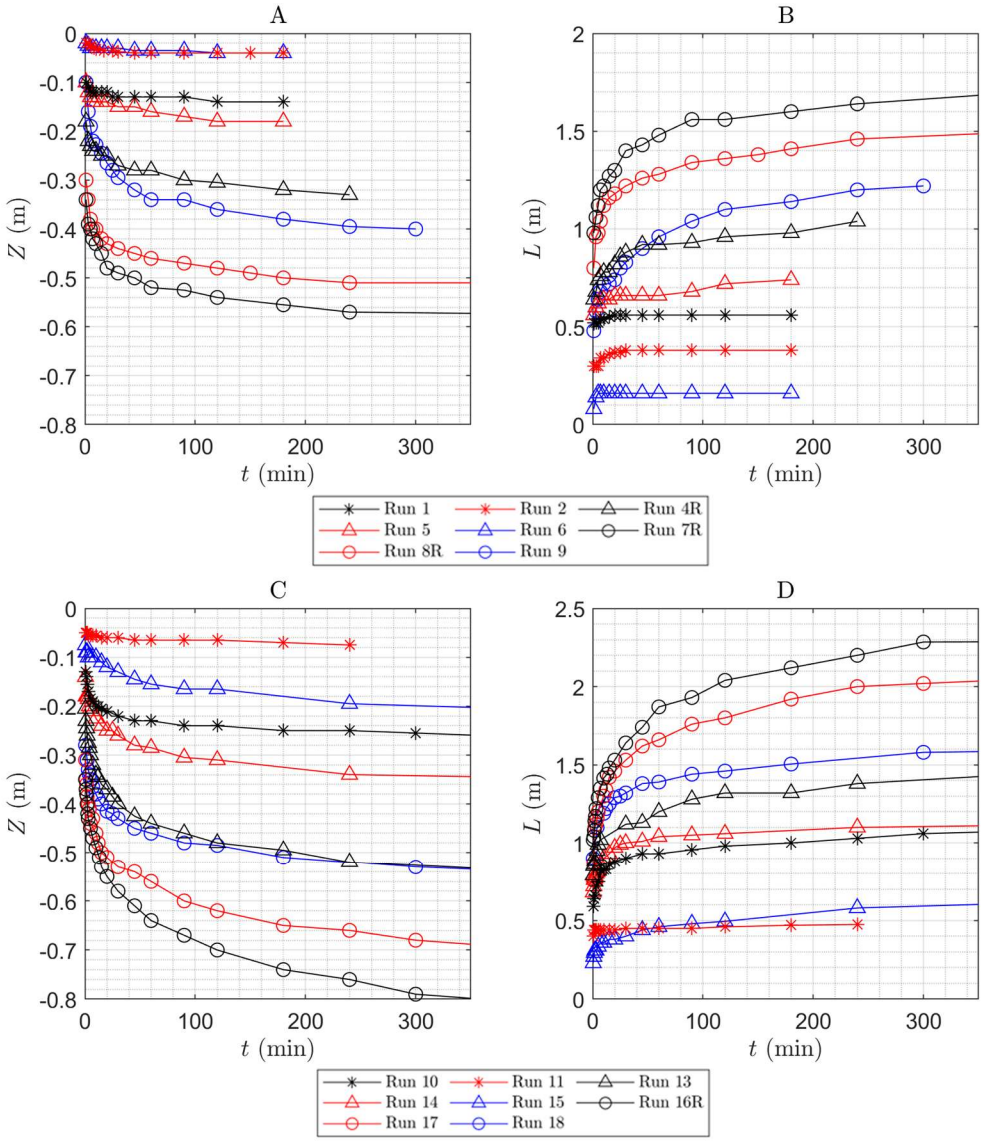

Fig. 19A-D. Observed scour depth with time (to 360 min) (A and C) and scour length with time (to 360 min) (B and D) for each flowrate material. Where A and B represent the coarse substrate and C and D represent the fine substrate. The most dramatic scour in both substrates occurs within the first 100 min of experimentation.

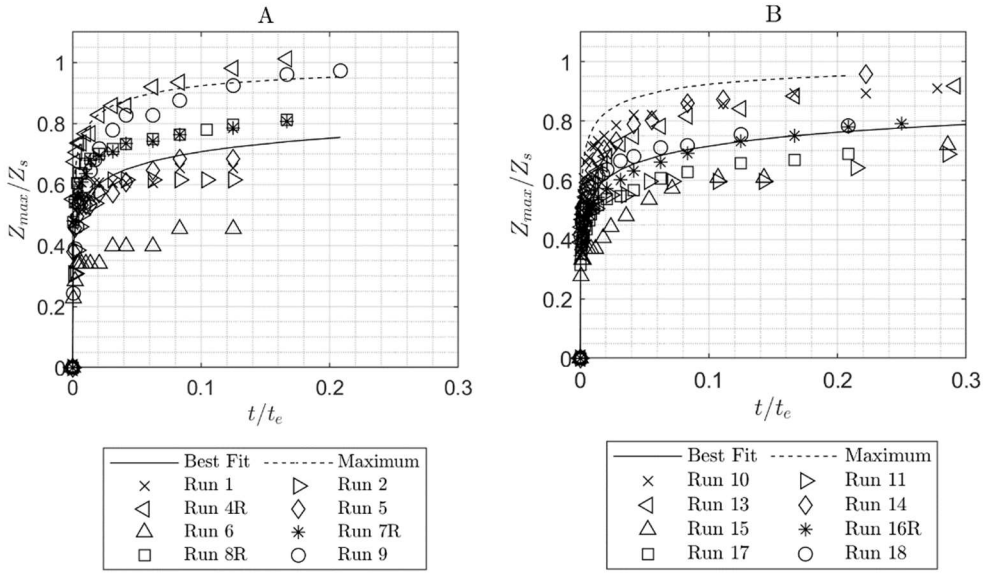

Fig. 20A and B. Time evolution prediction using Nasrollahi et al. (2008) method for (A.) coarse substrate and (B.) fine substrate.

Maximum Scour Prediction

For the current study a Z_{max} prediction method was developed for PK weirs. Eq. 2 was created to be an empirical equation and based on influential scour parameters (e.g. hydraulic, geometric, and substrate characteristics) to estimate Z_{max} downstream of PK weirs:

$$\frac{Z_{max}}{h_d} = \frac{K_l \left(\frac{q}{U_j W_o}\right)^m}{\left(\frac{H_d}{H_u}\right)^f \left(\frac{d_{50}}{P}\right)^p} \tag{2}$$

where coefficient $K_l = 6.9\Delta H - 0.39$, jet velocity $U_j = (2g\Delta H)$, ΔH = change in energy head upstream to downstream, total upstream head $H_u = H+P$, total downstream head $H_d = h_d + V^2/2g$, and constant coefficients $m = 1.09$, $f = 0.95$, and $p = 0.22$.

Equation 2 was developed using scour inducing variables that were based on hydraulic parameters collected during the experimental runs. The equation was based on

classical forms of scour prediction equations (such as Schoklitsch 1932 and Mason and Arumugam 1985), but incorporated unitless variable ratios. Each ratio was determined based on how one parameter affected the other variables' scour potential. For example, the H_d/H_u ratio represents how hydraulic parameters affect scour; as the H_u of the weir stayed constant with Q and H_d decreased with h_d, the result was an increase in scour potential. The unitless ratios were raised to coefficients m, f, and p. These coefficients were determined by setting $K_l = 1$ and solving the equation by changing the coefficient values until the same Z_{max} value observed is obtained. Once the coefficients for each run were determined, the m values for each run were averaged to obtain a singular value. This was repeated for the f and p coefficients. The average coefficients (m, f, and p) were applied to the unitless ratio. The equation was solved again for the observed Z_{max}, but with a varying K_l coefficient value. After the various K_l values were determined, they were plotted against the ΔH values and a linear trend emerged. The linear best fit line generated an equation for K_l as a function of ΔH (Fig. 21).

To predict Z_{max} for PK weirs, Eq. 2 and several prediction methods were juxtaposed to the experimental data presented herein (see Fig. 22). Schoklitsch (1932) developed a prediction method (Eq. 3) based on overflow flume experiments:

$$Z_{max} + h_d = \frac{4.75q^{0.57}\Delta h^{0.2}}{d_{90}^{0.32}} \quad (3)$$

where q = unit discharge (m^2/s), Δh = change in piezometric head level and piezometric tailwater level (m), and d_{90} = particle diameter (m) where 90% of substrate is smaller.

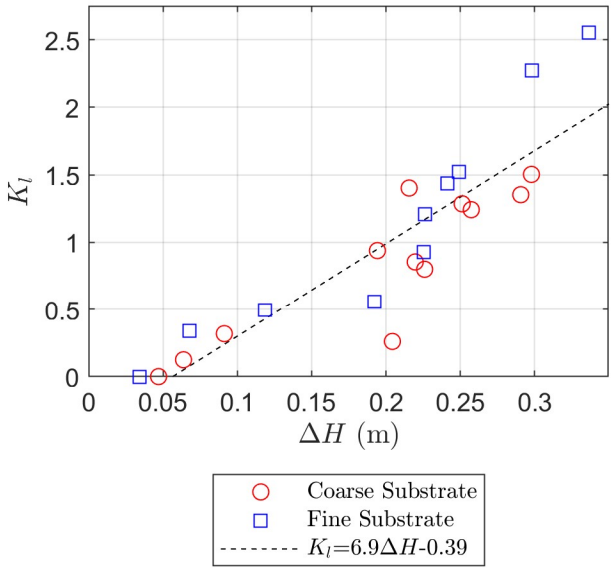

Fig. 21. General trend of K_l versus ΔH with a general trendline.

The Mason and Arumugam (1985) prediction method was developed for ski jump models and prototype structures (Eq. 4):

$$Z_{max} + h_d = \frac{K q^{a_m} \Delta h^c h_d^e}{g^k d_{50}^n} \tag{4}$$

where the coefficient $K = 6.42 - 3.1\Delta h^{0.1}$, $a_m = 0.6 - \Delta h/300$, $c = 0.15 + \Delta h/200$, $e = 0.15$, $k = 0.13$, and $n = 0.1$. Each of the given coefficients were determined by Mason and Arumugam (1985).

Bormann and Julien (1991) determined a scour prediction method for 2D jets at grade control structures (Eq. 5):

$$Z_{max} + P = \frac{K_b q^{0.6} U_j sin\theta}{(2Gg)^{0.8} d_{90}^{0.4}} \tag{5}$$

where P = drop height of the structure or weir height, $K_b = 1.8^2(\sin\phi/\sin(\phi+\theta)^{0.8}$, θ = jet angle, ϕ = angle of repose, and $g = 9.81$ m/s^2.

Jüstrich et al. (2016) formulated a maximum scour prediction specific to PK weirs (see Eq. 6):

$$\frac{Z_{max}}{d_{50}} = 0.42\left(\frac{h_c}{d_{50}}\right)^{1.7}\left(\frac{\Delta H}{h_d}\right)^{0.3} \quad (6)$$

where h_c = critical depth, $(q^2/g)^{1/3}$. The model size of the PK weir used by Jüstrich et al. (2016) was 0.15 m (approximately 3x smaller than the current study). Therefore, it was unclear what, if any, scale effects might be present between the two laboratory studies.

The final method compared herein is by Meftah and Mossa (2020) for various angled jets produced by grade control structures (Eq. 7):

$$\frac{Z_{max}}{h_u} = 0.24\left(1 + \frac{P}{h_u}\right)^{0.92}\left(\frac{h_d}{h_u}\right)^{0.24}\left(\frac{\theta}{\pi}\right)^{-0.34}(Fr_{sd})^{0.38} \quad (7)$$

where Fr_{sd} = densimetric Froude, $q/[h_u[(G\text{-}1)gd_{50}]^2]$.

Each predicted method was plotted against this data set to examine levels of agreement (Fig. 22) marked by a one-to-one ratio line and 20% variation bands.

Jüstrich et al. (2016), Mason and Arumugam (1985), and Eq. 2 had a coefficient of determination (R^2) of 0.96, 0.91, and 0.90, respectively and thus seem most suitable for predicting local scour at a PK weir. For this data, the accuracy of Jüstrich et al. (2016), Mason and Arumugam (1985), and Eq. 2 decreased for lesser Q and higher h_d. This may be attributed to the low scour volumes and the change in jet hydraulics due to high h_d. Additional research is needed for high h_d, although this may be of less interest to practitioners. For example, using the Jüstrich et al. (2016) prediction method with Q = 150 L/s and h_d = 0.257 m, the predicted Z_{max} is 0.12 m while the actual Z_{max} is 0.042 m. This method over predicts the value of Z_{max} by 185%. For high Q and low h_d, particularly

at Q = 600 l/s, the level of agreement between Jüstrich et al. (2016) and observed Z_{max} had a percent difference under 10%.

The prediction method for Eq. 2 had a maximum error of 288% difference for Q = 150 l/s and h_d = 0.26, and an overall average error for each particular run of about 39%. The level of agreement for Q = 600 l/s had a percent difference under 31%. Equation 2 was consistently more accurate for the fine substrate material and the average percent difference between the measurements taken from each substrate material was 17%. When Eq. 2 was applied to the scour data from Jüstrich et al. (2016), Eq. 2 could not accurately estimate Z_{max}.

The prediction method for Mason and Arumugam (1985) almost consistently overpredicted the, except for high Q and medium to low h_d conditions, where it then under predicted Z_{max}. It is estimated that this method begins to fall apart due to the k exponent (see Eq. 4). Meftah and Mossa (2019) method predicted that more scour would occur as particle size decreased, as h_d decreases, and as Q increases, but does not accurately predict Z_{max} for PK weirs. Furthermore, neither the Bormann and Julien (1991) or Schoklitsch (1932) methods could accurately predict Z_{max}. The method presented by Bormann and Julien (1991) may lack accuracy due to the K_b coefficient, and Schoklitsch (1932) significantly over estimates the amount of scour (Fig. 22).

Out of the various prediction methods that were evaluated, it was determined that the Jüstrich et al. (2016) prediction method was the most accurate for estimating maximum scour features downstream of a Type A (Pralong et al. 2011) PK weir.

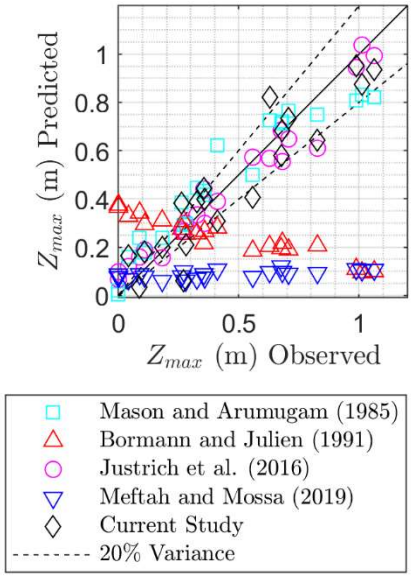

Fig. 22. Comparison of various literature prediction methods and actual measured values.

Conclusions

To summarize, local scour at non-linear weirs is an under-studied topic even with the growing popularity of these types of structures. Increased risk from climate change has made scour at a hydraulic structure a popular research topic for both researchers and practitioners.

It was concluded that under particular hydraulic conditions, scour at PK weirs can significantly exceed the P of the structure itself. The intensity, depth, and evolution of the scour morphology was dependent on particle characteristics, Q, and h_d. A decrease in particle size and h_d produced more scour. Whereas, an increase in Q increased the amount of scour.

Graphical results contained in the study can be used by practitioners as another method to estimate local scour at PK weirs. A combination of experimental observations and the Nasrollahi et al. (2008) time evolution prediction method was used to produce a

best fit line to help estimate the time evolution of scour at PK weirs under various hydraulic conditions.

There has been a significant amount of research pertaining to scour at different structures, which has produced various prediction methods. Eq. 2 was generated to predict scour and a select few scour prediction methods were evaluated within the study. It has been determined that the Jüstrich et al. (2016) prediction method was the most accurate and could estimate Z_{max} under various hydraulic conditions.

Different structures and projects have varying geometric and geological properties, which can cause the amount of scour to vary considerably from published data and prediction methods. Performing a physical model study of proposed projects and simulating particular hydraulic conditions is the only way to accurately understand the degree of scour that will occur.

Limitations of the study include steady-state hydraulic conditions (until a quasi-equilibrium state is achieved), three flow rates and tailwater conditions tested, and two relatively uniform substrate materials. One PK weir geometry was tested, and the results of this study can only be directly applied to horizontal downstream slopes. Even with the limitations, results can be used to determine conservative scour depths for scaled flows. Furthermore, the temporal evolution of scour results can determine scour evolution based on the length of the peak of a hydrograph. Finally, geologic material strength can be scaled using methods such as Annandale (1995) Erodibility Index, which can scale the strength of geologic material to the granular material tested in this study.

Data Availability Statement

Some or all data, models, or code that support the findings of this study are available from the corresponding author upon reasonable request.

Acknowledgements

This study was funded by the State of Utah through the Utah Water Research Laboratory and by a United States Geological Survey (USGS) 104B grant.

APRON AND CUTOFF WALL SCOUR PROTECTION FOR PIANO KEY WEIRS

Abstract

Piano key weirs are used in a variety of flow control structure applications including as spillway crests and open channel diversion structures. However, structure-specific design guidance for scour mitigation is needed in the consideration of a horizontal apron with a cutoff wall. For this reason, a large-scale physical model study is performed to evaluate how various apron lengths reduce downstream maximum scour depths, scour hole lengths, and volume of material for different hydraulic conditions. It is determined that a horizontal apron deflects the jets from the piano key weir in the horizontal direction, thus significantly reducing scour. Of the three apron lengths, a length 1.5 times the weir height reduces scour by 75% on average with marginal reduction in scour for longer aprons. Equations are created to help practitioners to estimate apron length, scour depth downstream of the apron, and cutoff wall depth.

Keywords: piano key weir, local scour, scour countermeasure, downstream apron

Introduction

When considering current design standards, sustainability principles, and observed trends in flooding, it is evident that estimating local scour and appropriate countermeasures at hydraulic structures is a challenging task. This is due to catchment-based processes (Zehe et al. 2005) (e.g. runoff hydrographs, river morphology, and transport of sediments, and debris) along with structure-based processes (Ettema et al. 2004) including the flow field, resistance of local sediments and local geology, and scour evolution leading to damage or even failure of the structure (Laursen 1952, Bombardelli

et al. 2018, Palermo et al. 2020b). Weirs are a common hydraulic structure found in rivers and incorporated in dams and levees. Often, local scour occurs at weirs due to the falling nappe or the jet generated by the geometry of the weir. Jets are characterized based on the jet angle or orientation, on flow field characteristics (2D or 3D jets), and whether they are plunging or submerged (e.g., Hoffmans and Verheij 1997, Adduce and Sciortino 2006, Dey and Raikar 2007, Bombardelli et al. 2018, Ben Meftah and Mossa 2020, Lantz et al. 2020, Palermo et al. 2020b).

Scour is a frequent topic in research with numerous publications focused on drop structures, including linear weirs. However, scour has been minimally researched for piano key (PK) weirs, until recently. During the short history of PK weir use, structures have been designed and constructed in Asia, Australia, Europe, and North America such as the run-of-river Van Phong PK weir in Vietnam (Ho Ta Khanh et al. 2011, Crookston et al. 2019, UEE 2021). Piano key weirs perform well as in-channel flow control structures due to their hydraulic efficiency, passive flow control nature, construction economy, and ability to pass floating debris (Schleiss 2011, Ribeiro et al., 2012, Machiels et al. 2014, López-Soto et al. 2016). In recent years, there has been increased interest regarding scour morphology at PK weirs (Laugier et al. 2013, Jüstrich et al. 2016, Pfister et al. 2017, Lantz et al. 2020, Lantz 2021). It is understood that PK weir geometries produce multiple discharge jet angles (near-vertical and sub-vertical) that can create local scour at the toe of a PK weir (Pfister et al. 2017, Palermo et al. 2020a, Yazdi et al. 2021) with a prediction method by Jüstrich et al. (2016) to estimate scour geometry. However, the authors are aware of only one study on scour mitigation (via rip-rap, Pfister et al. 2017) specific to PK weirs.

Scour protection at stilling basins and other common terminal structures is usually based on site-specific studies and design manuals. Some design manuals that are frequently used is the United States Department of the Interior Bureau of Reclamation (USBR) *Engineering Monograph No. 25: Hydraulic Design of Stilling Basins and Energy Dissipators*, the Federal Highway Administration (FHWA): *Hydraulic Engineering Circular No. 14: Hydraulic Design of Energy Dissipators for Culverts and Channels*, and the United States Department of Agriculture's (USDA) *The SAF Stilling Basin.* Other design manuals include Hoffmans and Verhfi's *Scour Manual*, Vischer and Hager's *Energy Dissipators: IAHR Hydraulic Structures Design Manuals 9*, Novark et al.'s *Hydraulic Structures*, and Khatsuria's *Hydraulics of Spillways and Energy Dissipators*. Design manuals are great resources to help engineers face multiple challenges encountered in different engineering projects. Still, structure-specific guidance is needed for techno-economical solutions, particularly for smaller projects without the budget for numerical or physical model studies.

Current design guidance for scour mitigation at PK weirs consists of two articles. Pfister et al. (2017) focused on the design of a pre-excavated rip-rap apron based on the Jüstrich et al. (2016) prediction method, which follows the dimension of a scour hole if the structure had no protection. Ho Ta Khanh et al. (2011) concluded that tall (e.g. > 50 m) PK weirs in rivers only need a short stilling basin, end sill, and stepped outlet key to dissipate energy. There is no research pertaining to aprons as a form of scour mitigation downstream of PK weirs. Aprons are a simple and cost-effective alternative for scour mitigation.

Cutoff walls are commonly included with concrete aprons to prevent a failure mode via undermining of the slabs (Hassan and Narayanan 1985, Chatterjee et al. 1994, Sarkar and Dey 2005, Dey and Sarkar 2006). Published literature references a maximum scour depth and an additional factor of safety for sizing cutoff walls, or keying in the cutoff wall into resilient rock. Moreover, there is currently no PK weir literature available for the design of a cutoff wall for scour mitigation.

Therefore, a large-scale physical model study is performed at Utah State University to analyze scour mitigation via various lengths of horizontal aprons with cutoff walls for two non-cohesive substrate materials.

Experimental Setup

For this study, a rectangular flume was constructed at the Utah Water Research Laboratory (16-m long, 2-m wide, and 1.8-m deep) with a transparent acrylic wall section to observe scour morphology and protection. The flume provided uniform flows in the headbox to a Type A (Pralong et al. 2011) PK weir via a diffuser pipe and rock baffling. The 4-key acrylic PK weir dimensions are summarized in Fig. 23 and Table 11 where B = depth of the PK weir, B_b = streamwise length of the base of the PK, B_i = the length of the inlet key, B_o = the length of the outlet key, S_o = slope of the outlet key, S_i = slope of the inlet key, W_u = cycle width, N = number of cycles, P = weir height, T_s = sidewall thickness, W_i = width of the inlet key, W_o = width of the outlet key, and P_d = height of the PK weir base relative to the invert of the channel. Note that a false floor was not included upstream of the PK weir, as its presence would be negligible on the results of this study (see Fig. 23).

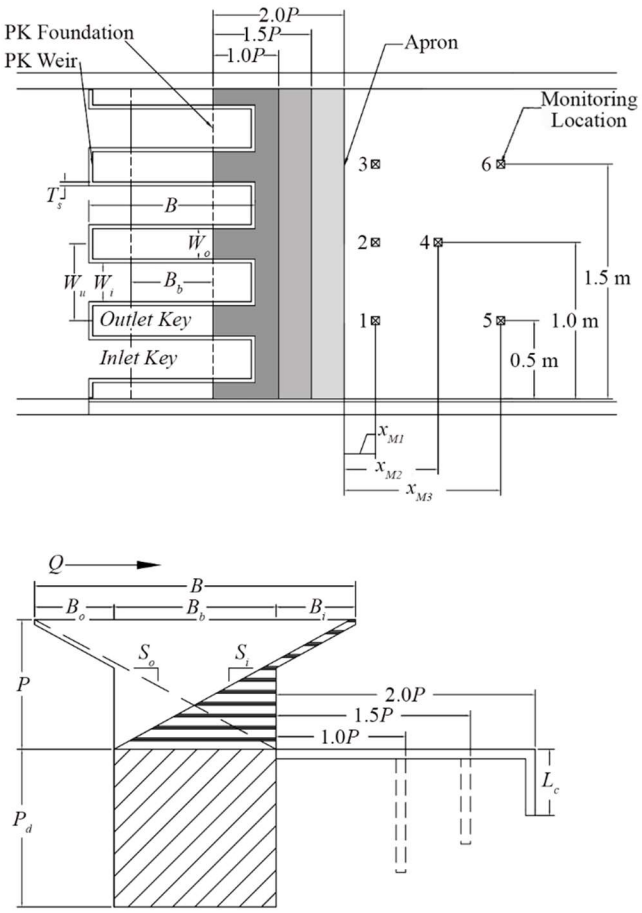

Fig. 23. Plan and profile view of weir dimensions and flume set up.

The various apron lengths and cutoff walls were fabricated using dimensional lumber and coated for waterproofing. When the aprons were installed, they were leveled at the elevation of the base of the PK weir. Additionally, a stop log assembly was installed at the end of the flume to control tailwater elevations.

This study included two non-cohesive gravel substrates. Both substrate materials had a uniform gradation, or a similar particle size throughout the gradation. The first substrate material was a coarse gravel with d_{90} = 20.00 mm, d_{50} = 13.00 mm, gradation coefficient σ = 1.54, density ρ = 2604.28 kg/m^3, specific weight γ = 25,547.98 N/m^3, and specific gravity G = 2.61, where d_{xx} is the diameter of which xx% is finer. The first

substrate material was referred to as the coarse substrate. The second substrate material was a fine gravel with d_{90} = 9.10 mm, d_{50} = 6.50 mm, coefficient of gradation σ = 1.30, ρ = 2604.28 kg/m^3, γ = 25,547.98 N/m^3, and G = 2.61. The second substrate material was referred to as the fine substrate material. The substrate material was uniformly placed as a planar bed with an elevation corresponding to the base of the PK weir.

Table 11 – Experimental PK dimension summary.

Parameter	Value
B	1.04 m
B_b	0.52 m
$B_i = B_o$	0.26 m
S_o=S_i	0.55
W_u	0.49 m
N	4.00
P	0.42 m
T_s	.025 m
W_i/W_o	1.28
Crest Type	Flat
P_d	1.09 m

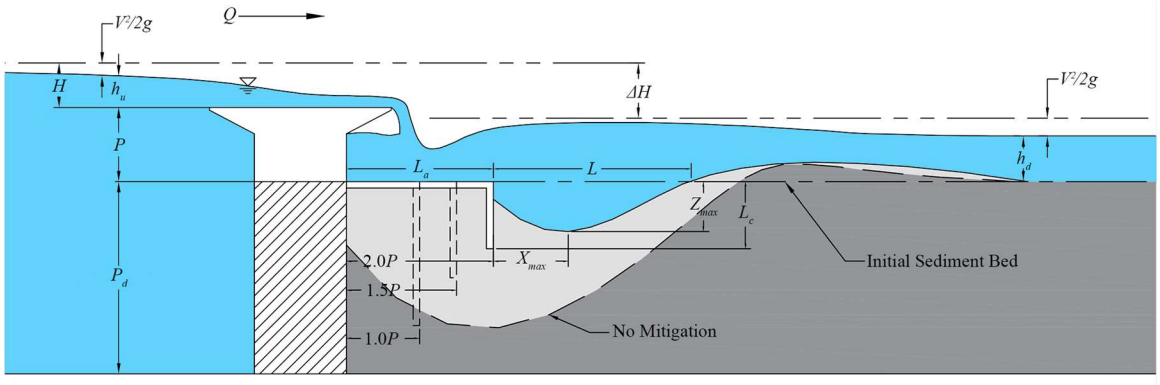

Fig. 24. Profile of experimental setup with key parameters used in this study.

A calibrated venturi meter (±0.25%) was used to measure flow rate (Q). A point gauge (±0.75 mm) with a stilling well, hydraulically connected two meters upstream of

the weir, measured upstream piezometric head. An ultra-sonic sensor (±1%) was used to measure the dynamic downstream piezometric head, which is a measure of the tailwater depth (h_d) (Microsonic 2021, Zhang et al. 2018).

An important aspect of this study was to document scour morphology with and without the apron and cutoff wall. Therefore, two techniques were used to estimate the temporal evolution of the scour hole. As shown in Fig. 23, columns of low-buoyancy spheres (G = 0.53) were spaced vertically in the substrate at 0.1 m in columns (± 12 mm). Sphere column location was color coded and the specific weight of the spheres was adjusted so that spheres would stay buried until approximately half of the sphere was exposed. Once the sphere was uncovered to this point, the sphere quickly rose to the water surface for documentation (video recording).

To determine ultimate scour dimensions and bed topography, the substrate was scanned with an Intel RealSense D435 depth camera (± 0.001 m) (Intel 2021, Bung et al. 2020) processed with a USU custom MATLAB script. This camera is capable of capturing the surface of solids or even rapidly varied flow water surfaces in three dimensions; camera specifications are summarized in Table 12. Post-processing included 2D and 3D scour morphology plots to quantify maximum scour location (Z_{max}), distance of Z_{max} from the weir in the streamwise direction (X_{max}), maximum length of the scour hole (L_{max}), and other scour features.

Each of the four apron lengths (L_a) 0P, 1P, 1.5P, and 2P, were tested for three different Q with the lowest permissible corresponding tailwater depth (h_d) (Table 13). Each test began by slowly filling the headbox and substrate box until the weir was in a submerged condition. The target Q was set, the h_d was then lowered to the lowest

Table 12 – Intel RealSense D435 specifications.

Feature	Detail
Global Shutter	3µm × 3µm pixel size
IR Stereo: FOV	86°×57° (±3°)
IR Stereo: Resolution	1280×720
RGB: FOV	64°×41°×77° (±3°)
RGB: Resolution	1920×1080

permissible depth, and then the timer and video recording array were initiated. Note that for certain values of Q the horizontal bed prevented the target h_d (0.33P) from being achieved. Multiple experiments were conducted for more than 18 hours each to confirm equilibrium conditions and necessary durations for the remainder of the test matrix.

Table 13 – Test matrix for the current study for the coarse and fine substrate.

Substrate Type	Discharge	Headwater	Tailwater	Apron Length
d_{50} = 6.5 mm d_{50} = 13 mm	150 l/s	$H/P \approx 0.11$	$0.3P \approx 14$ cm	$2.0P = 0.84$ m
				$1.5P = 0.63$ m
				$1.0P = 0.42$ m
	300 l/s	$H/P \approx 0.18$	$0.3P \approx 14$ cm	$2.0P = 0.84$ m
				$1.5P = 0.63$ m
				$1.0P = 0.42$ m
	600 l/s	$H/P \approx 0.35$	$0.3P \approx 14$ cm	$2.0P = 0.84$ m
				$1.5P = 0.63$ m
				$1.0P = 0.42$ m

Results

Hydraulic Observations

The PK weir geometry creates a 3D flow field that can be characterized by near-vertical and oblique plunging jets exiting the inlet and outlet keys, respectively. The

oblique jet had a larger unit discharge than the near-vertical jet, which resulted in a greater potential for scour. With no scour protection measures, both jets impinge on the planar gravel bed with a rapid initial scour phase (Lantz 2020). The primary advantage of the horizontal apron was the deflection of both jets towards the direction of flow allowing some jet diffusion along the length of the apron (Fig. 25). Depending upon the value of Q, the flows exiting the horizontal apron impart sufficient shear stress to cause local scour, confirming the need for a cutoff wall to avoid this failure scenario.

Fig. 25A and B. Run 14 (A) in comparison to Run 23 (B) for the fine substrate, Q =300 l/s, and h_d = 0.17 m (Table 4). Run 23 has significantly less scour due to L_a = 2.0P.

Local Scour

The overall observed trend was that scour depth and maximum scour dimensions decrease non-linearly with increasing L_a for a given Q. (Fig. 26 and Table 14). The percent reductions attributed to an L_a, relative to the no protection scenario, are presented in Fig. 27.

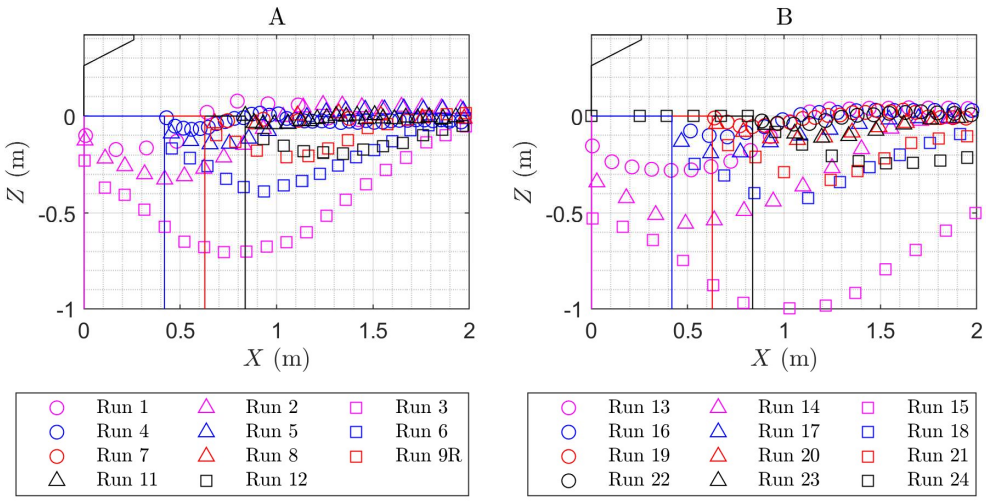

Fig. 26A and B. 2D maximum scour profiles for various L_a and Q for (A) the coarse substrate and (B) fine substrate. Run numbers are associated with Table 14. Note that the sediment bed was deeper than 1 m.

It was observed that by adding a 1.0P horizontal apron that the Z_{max} was reduced by about 56% for Q = 600 l/s and an average reduction for all flows of 57%. Increasing the L_a to 1.5P reduced Z_{max} by an average of 75%, and by adding a 2.0P apron Z_{max} was reduced by an average of 83% (Table 14 and Fig. 27A and B). The change in scour depth

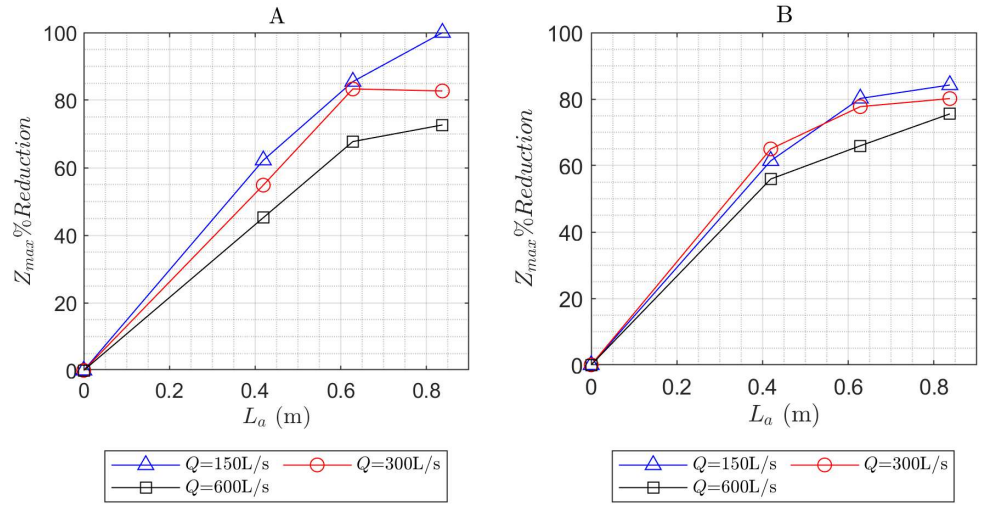

Fig. 27A and B. Reduction in scour with increased L_a for (A) coarse substrate and (B) fine substrate.

from the 1.5*P* to the 2.0*P* apron was on average 8%, thus from these laboratory observations additional protection from a conservatively long L_a may only minimize scour marginally. Fig. 28(A and B) corroborate that as L_a increases Z_{max} decreases. Similar to Z_{max}, the varying L_a also affected L_{max} [Fig. 29(A and B)]. For the coarse substrate material, L_{max} decreased as L_a increased for all Q (Fig. 29A). For the fine substrate material, L_{max} decreased relative to the no apron condition, but for larger Q the

Table 14 – Testing values for each experimental run.

Run #	***d_{50}*** **(mm)**	***t*** **(min)**	***La*** **x*P***	**(m)**	***Q*** **(l/s)**	***q*** **(m^2/s)**
1	13.00	180.00	0.0P	0.00	150	0.08
2	13.00	240.00	0.0P	0.00	300	0.15
3	13.00	900.00	0.0P	0.00	600	0.30
4	13.00	360.00	1.0P	0.42	150	0.08
5	13.00	360.00	1.0P	0.42	300	0.15
6	13.00	870.00	1.0P	0.42	600	0.30
7	13.00	360.00	1.5P	0.63	150	0.08
8	13.00	360.00	1.5P	0.63	300	0.15
9	13.00	360.00	1.5P	0.63	600	0.30
9R	13.00	360.00	1.5P	0.63	600	0.30
10*	13.00	no scour	2.0P	0.84	150	0.08
11	13.00	120.00	2.0P	0.84	300	0.15
12	13.00	360.00	2.0P	0.84	600	0.30
13	6.50	450.00	0.0P	0.00	150	0.08
14	6.50	1050.00	0.0P	0.00	300	0.15
15	6.50	1170.00	0.0P	0.00	600	0.30
16	6.50	840.00	1.0P	0.42	150	0.08
17	6.50	780.00	1.0P	0.42	300	0.15
18	6.50	720.00	1.0P	0.42	600	0.30
19	6.50	240.00	1.5P	0.63	150	0.08
20	6.50	840.00	1.5P	0.63	300	0.15
21	6.50	990.00	1.5P	0.63	600	0.30
22	6.50	480.00	2.0P	0.84	150	0.08
23	6.50	600.00	2.0P	0.84	300	0.15
24	6.50	720.00	2.0P	0.84	600	0.30

*No observed scour

L_{max} increased as L_a increased (Fig. 29B). The L_{max} increased because the apron transferred the sub-vertical jets to horizontal jets. This causes less energy to be transferred vertically into the bed, causing increased shear stress on the top layers of the bed material. Increased shear stress causes the scour hole length to increase. To summarize, the horizontal jet produces a shallow long scour hole for higher *Q*s. However, for higher *Q*s, an apron may not be sufficient to prevent all scour. (Fig. 28A-D).

Table 15 – Measured experimental values

Run #	h_d **(m)**	Z_{max} **(m)**	X_{max} **(m)**	L_{max} **(m)**	~~**V**~~ **(m^3)**
1	0.16	-0.18	0.21	0.61	0.12
2	0.17	-0.33	0.42	1.07	0.36
3	0.22	-0.71	0.69	2.20	1.49
4	0.09	-0.07	0.11	0.47	0.03
5	0.16	-0.15	0.22	0.75	0.12
6	0.21	-0.39	0.51	1.54	0.50
7	0.10	-0.03	0.1	0.31	0.00
8	0.17	-0.06	0.18	0.44	0.03
9	0.22	-0.28	0.53	1.54	0.37
9R	0.23	-0.23	0.52	1.45	0.37
10*	0.09				
11	0.15	-0.06	0.16	0.36	0.02
12	0.22	-0.19	0.42	1.18	0.27
13	0.10	-0.28	0.4	1.07	0.39
14	0.14	-0.56	0.52	1.81	1.03
15	0.22	-1.01	1	3.19	3.36
16	0.11	-0.11	0.27	0.61	0.07
17	0.16	-0.2	0.25	1.15	0.26
18	0.24	-0.45	0.63	1.83	0.74
19	0.11	-0.06	0.22	0.47	0.03
20	0.15	-0.12	0.39	1.28	0.15
21	0.25	-0.34	0.49	2.37	0.56
22	0.10	-0.04	0.18	0.45	0.02
23	0.15	-0.11	0.37	1.02	0.12
24	0.24	-0.25	0.77	3.05	0.45

*No observed scour

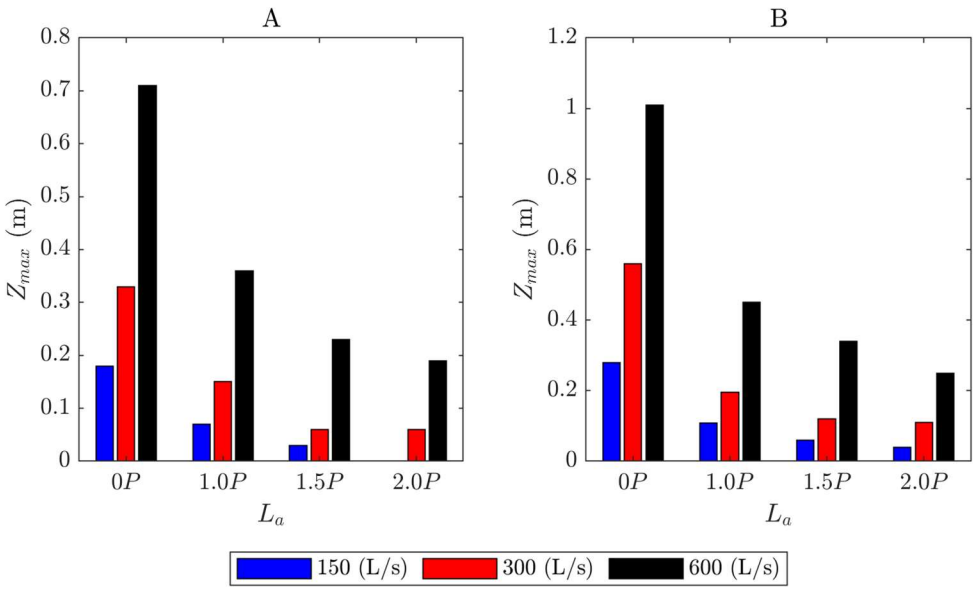

Fig. 28A and B. A graphical view of the effects L_a has on Z_{max} for (A) coarse substrate and (B) fine substrate.

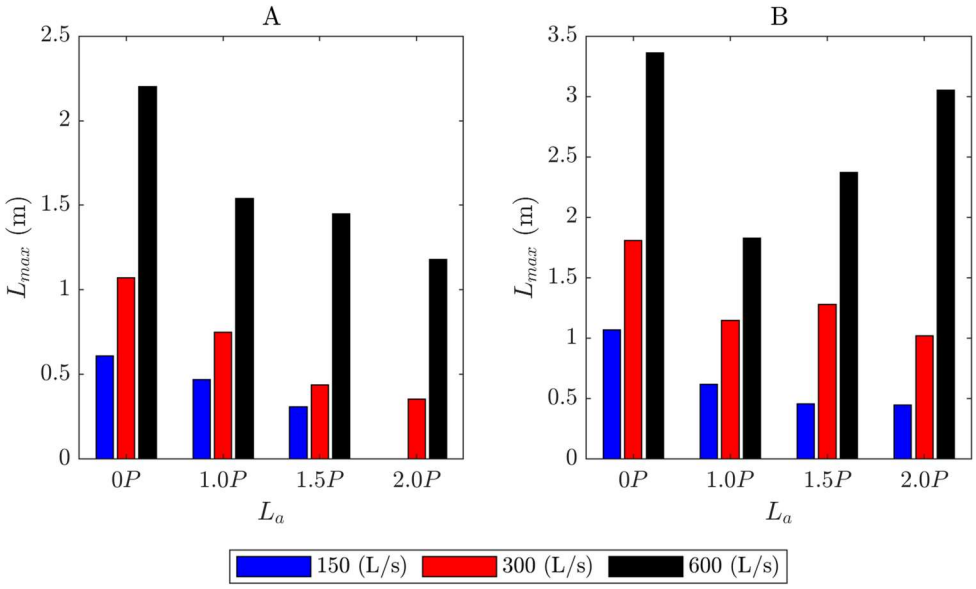

Fig. 29A and B. A graphical view of the effects L_a has on the L_{max} for (A) coarse substrate and (B) fine substrate.

Horizontal Apron Design Guidance

The proper design of an apron and cutoff wall can help protect run-of-river structures from detrimental scour events associated with hydraulic conditions during

flood events. From this study it was observed that there was an average change of 13.83% difference between 1.0P and 1.5P apron sizes and 7.93% difference between 1.5P and 2.0P apron lengths in the amount of Z_{max} observed. A relatively minimal change in scour depth was observed between the inclusion of an apron versus no apron. Therefore, an adequate apron size would be an L_a = 1.5P to mitigate the majority of scour.

Eq. 8 is proposed for approximating L_a and was adapted to this study from Jüstrich et al. (2016):

$$L_a = xP = Z_{pre}\left(\frac{L_{pre}}{X_{pre}}\right)^q \tag{8}$$

where x = non-dimensional multiplier, maximum predicted scour Z_{pre} = $[0.42(h_c/d_{50})^{1.7}(\Delta H/h_d)^{0.3}]d_{50}$, critical depth $h_c = (q^2/g)^{1/3}$, q = unit discharge, g = acceleration due to gravity, ΔH = change in energy head, h_d = tailwater depth, predicted location of maximum scour in streamwise direction $X_{pre} = 1.20Z_{pre} + (B_i/2)$, B_i =depth of inlet key, and predicted maximum scour length $L_{pre} = 2.70Z_{pre} + B_i$ (Jüstrich et al. 2016).

Eq. 8 considers hydraulic and substrate variables (e.g. d_{50}, ΔH, h_c, and weir geometry), which contrive Jüstrich et al. (2016)'s prediction equations. Furthermore, Eq. 8 is only an approximation for L_a that will reduce the amount of scour downstream of a PK weir under steady-state, equilibrium conditions.

Once an apron design length (L_{design}) is selected, Eq. 9 can be used to estimate the Z_{max} downstream of the apron.

$$Z_{max} = h_c\left(\frac{Z_{pre}}{L_{design}}\right) \tag{9}$$

It was observed that the equation becomes more accurate as both Q and L_a increase. Predicted scour depths are plotted against actual scour depths with a coefficient of determination (R^2) = 0.94, a one to one ratio, and 20% variation bands (Fig. 30).

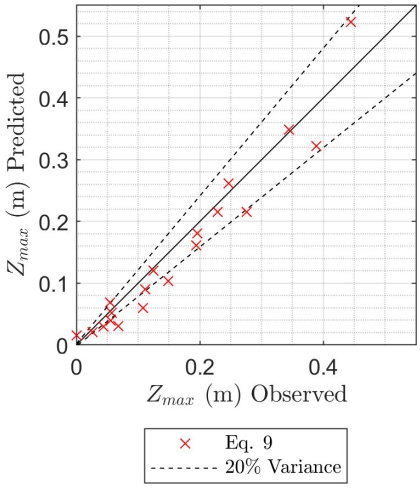

Fig. 30. Predicted Z_{max} plotted against observed Z_{max} downstream of L_a.

Cutoff Wall Design

Often, a cutoff wall is included at the end of a concrete apron or slab to protect against undermining. Selecting a cutoff wall depth (L_c) often considers an estimation of Z_{max} (either with protection or without protection) and local geology, for example, if competent rock is near the slab it may be economically viable to key into this layer. For PK weirs there was no published design guidance for estimating L_c, but for certain conditions significant scour could occur at the structure foundation (Jüstrich et al. 2016; Lantz et al. 2020; Pfister et al. 2017). Therefore, Eq. 10 was developed to estimate the cutoff wall length for PK weirs:

$$L_c = F.S.\left(Z_{max} + \left(\frac{H}{h_d}\right)P\right) \tag{10}$$

where $F.S.$ = factor of safety, and H = total energy head relative to the weir crest.

Eq. 10 uses the Z_{max} downstream of an apron and the ratio of H to h_d, which considers the hydraulic conditions that will occur at the structure. For example, if the h_d was generally high and the H was low then the contribution of the hydraulics will not likely affect the amount of scour. A factor of safety can be added to the cutoff wall equation depending on other site-specific factors and engineering judgement, as this may be considered as a minimum cutoff wall-length.

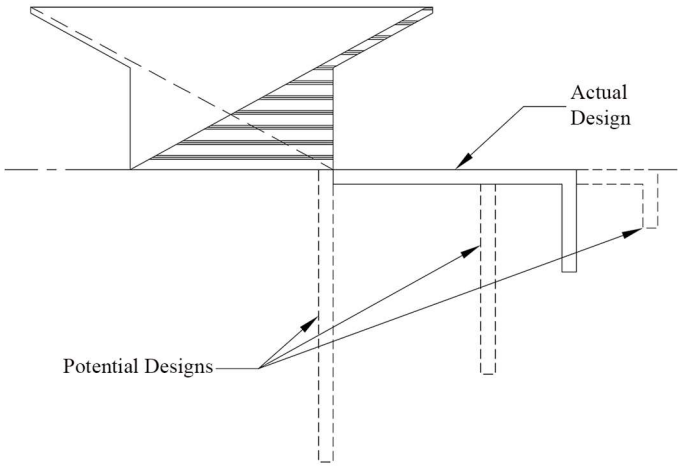

Fig. 31. Scour mitigation options.

Conclusions

Limited published guidance is available to estimate local scour downstream of PK weirs, with no design guidance available on minimal apron and cutoff wall lengths. This encouraged a large-scale physical model study on the effects of scour at PK weirs with and without aprons and cutoff walls. From this study the following conclusions have been made:

- Jets ensuing from the PK weir structure diffuse over the apron and cause horizontal jet scour downstream of the apron.
- Adding a 1.0P long apron can reduce scour by an average of 61%, adding a 1.5P long apron scour can be reduced by an average of 75%, and adding a 2.0P apron it can reduce scour by an average of 83%.
- Equations were created to estimate L_a, Z_{max} downstream of an apron, and L_c to protect the structure from scour undermining.
- For this study, it was determined that there was 8% difference in the reduction of scour from a 1.5P apron length to a 2.0P apron length, and a 1.5P apron may be an adequate and cost-effective length to minimize scour. Note that as the substrate diameter decreases the potential for scour depth and length downstream of the apron will increase.

There are multiple limitations to this study, but there are ways that practitioners can overcome the limitations. First, the steady-state nature of the testing. To overcome this limitation, practitioners can use Z_{max} values as conservative design values. Another limitation was the that only three Q and one h_d conditions were tested in this study. To overcome this limitation, practitioners could use graphical means to interpolate potential Z_{max} values based on the rating curves provided. Furthermore, only two relatively uniform substrate materials were studied. Practitioners could use methods similar Annadale (1995) Erodibility Index method to scale geologic material strength to a similar material that was tested in the study. Additionally, these results and equations only directly apply to horizontal downstream slopes. Lastly, only one PK weir geometry was tested.

CONCLUSIONS

The purpose of this study was to better understand the geometric and hydraulic effects that PK weirs have on scour morphology. This study helps give practitioners guidance on the design of aprons downstream of PK weirs. Designers should take into consideration the effect that PK weirs have on local scour. The following conclusions are based on the results of this study:

- Hydraulic conditions can significantly change scour morphology and scour intensity. Scour effects intensify as flow rate increases and decrease as tailwater depth increases. Additionally, smaller substrate particles produce increased scour effects.
- Of the various scour prediction methods analyzed, the prediction method of Jüstrich et al. (2016) is the most accurate and comprehensive method developed to predict local scour downstream of PK weirs.
- The time evolution of scour method developed by Nashrollahi et al. (2008) can be used to estimate the amount of scour and time it takes to reach equilibrium based on laboratory observations from this study.
- It was determined that by adding an apron length of 1.0P, Z_{max} can be reduced on average 57%. The reduction of Z_{max} increases asymptotically as apron length increases, particularly as Q increases and d_{50} decreases. Additionally, it was determined that the percent difference in change of apron length from 1.5P to 2.0P was small enough that a 1.5P apron length would be a cost-effective length to use for this PK weir configuration.

- Equations have been generated to help design apron lengths and cutoff wall depths downstream of PK weirs. Equations to estimate scour downstream of an apron were used to help in the design of cutoff wall length.

REFERENCES

Aderibigbe, O., and Rajaratnam, N. 2006. “Effect of sediment gradation on erosion by plane turbulent wall jets.” *J. Hydraul. Eng*. 1034–1042. DOI: 10.1061/(ASCE)0733-9429(1998)124:10(1034).

Adduce, C., and Sciortino, G. 2006. “Scour due to a horizontal turbulent jet: Numerical and experimental investigation.” *J. Hydraul. Res*. 44(5). 663–673.

Annandale, G. W. 1995. “Erodibility.” *J. Hydraul. Res.* 33(4), 471–494. DOI: 10.1080/00221689509498656.

Meftah, B. M., and Mossa, M. 2020. “New Approach to Predicting Local Scour Downstream of Grade-Control Structure.” *J. Hydraul. Eng*. 146(2). DOI: 10.1061/(ASCE)HY.1943-7900.0001649.

Bombardelli, F. A., Palermo, M., and Pagliara, S. 2018. “Temporal evolution of jet induced scour depth in cohesionless granular beds and the phenomenological theory of turbulence.” *Physics of Fluids*. 30(8), 085109. DOI: 10.1063/1.5041800.

Bormann, N. E., and Julien, P. Y. 1991. “Scour Downstream of Grade-Control Structures.” *J. Hydraul. Eng*. 117(5). 579–594. DOI: 10.1061/(ASCE)0733-9429(1991)117:5(579).

Bung, D. B., Crookston, B. M., Valero, D. 2020. “Turbulent free-surface monitoring with an RGB-D sensor: the hydraulic jump case.” *J. Hydraul. Res*. 1-12. DOI: 10.1080/00221686.2020.1844810.

Center for Disaster Philanthropy. 2019. "2019 Catastrophic River Flooding.” *2019 Catastrophic River Flooding - Center for Disaster Philanthropy.* Accessed Jan. 25, 2020. <https://disasterphilanthropy.org/disaster/2019-u-s-spring-floods/>

Chatterjee, S. S., Ghosh, S. N., and Chatterjee, M. 1994. "Local Scour due to Submerged Horizontal Jet." *J. of Hydraul. Eng*. 120(8), 973–992. DOI: 10.1061/(ASCE)0733-9429(1994)120:8(973).

Chen, J., Hsu, H., and Hong, Y. 2016. "The influence of upstream slope on the local scour at drop structure." *J. Mt. Sci.* 13(12). 2237-2248. DOI:10.1007/s11629-015-3790-5.

Crookston, B. M., Erpicum, S., Tullis, B. P., and Laugier, F. 2019. "Hydraulics of Labyrinth and Piano Key Weirs: 100 Years of Prototype Structures, Advancements, and Future Research Needs." *J. Hydraul. Res*. 145(12). 02519004. DOI: 10.1061/(ASCE)HY.1943-7900.0001646.

Dey, S., and Raikar, R. V. 2007. "Scour below a High Vertical Drop." *Journal of Hydraulic Engineering*, 133(5), 564–568. DOI: 10.1061/(ASCE)0733-9429(2007)133:5(564).

Dey, S., and Sarkar, A. 2006. "Scour Downstream of an Apron Due to Submerged Horizontal Jets." *J. Hydraul. Eng.* 132(3). 246–257. DOI: 10.1061/(ASCE)0733-9429(2006)132:3(246).

Elnikhely, E. A., and Fathy, I. 2020. "Prediction of scour downstream of triangular labyrinth weirs." *Alexandria Engineering Journal*. 59(2). 1037–1047. DOI: 10.1016/j.aej.2020.03.025.

Ettema, R., Yoon, B., Nakato, T., and Muste, M. 2004. "A review of scour conditions and scour-estimation difficulties for bridge abutments." *Water Eng.* 8(6). 643–650. DOI: 10.1007/BF02823555.

FloodList. 2020. “Floods in USA.” Accessed: Jan. 25, 2020. <http://floodlist.com/america/usa>

Gebhardt, M., Herbst, J., Merkel, J., and Belzner, F. 2019. “Sedimentation at labyrinth weirs – an experimental study of the self-cleaning process.” *J. Hydraul. Res*. 57(4). 579–590. DOI: 10.1080/00221686.2018.1494053.

Green, C. 2010. “Towards sustainable flood risk management.” *Int. J. Disaster Risk Sci.* 1(1). 33-43. DOI: 10.3974/j.

Hassan, N. M. K. N., and Narayanan, R. 1985. “Local Scour Downstream of an Apron.” *J. Hydraul. Eng*. 111(11). 1371–1384. DOI: 10.1061/(ASCE)0733-9429(1985)111:11(1371).

Ho Ta Khanh, M., Truong, C. H., and Nguyen, T. H. 2011. “Main Results of the P.K weir model tests in Vietnam (2004-2010).” *Labyrinth and Piano Key Weirs: PKW 2011*. 191–198. London, UK:Taylor and Francis Group.

Hoffmans, G. J. C. M., and Verheij, H. J. 1997. *Scour Manual*. Balkema, Rotterbam, The Netherlands.

Jia, Y., Kitamura, T., and Wang, S. S. Y. 2001. “Simulation of Scour Process in Plunging Pool of Loose Bed-Material” *J. Hydraul. Eng*. 127(3). 04016043. 219-229. DOI: 10.1061/(ASCE)0733-9429(2001)127:3(219).

Intel. 2021. “Depth Camera D435.” *Intel RealSense*. Accessed: Mar. 4, 2021 <https://www.intelrealsense.com/depth-camera-d435/>

Jüstrich, S., Pfister, M., and Schleiss, A. J. 2016. “Mobile Riverbed Scour Downstream of a Piano Key Weir.” *J. Hydraul. Eng*. 142(11). 04016043. DOI: 10.1061/(ASCE)HY.1943-7900.0001189.

Khatsuria, R. M. 2005. *Hydraulics of Spillways and Energy Dissipators.* New York, NY: Marcel Decker.

Kuhnle, R. A., Alonso, C. V., and Shields, F. D. 2002. "Local Scour Associated with Angled Spur Dikes." *J. Hydraul. Eng*. 128(12). 1087–1093. DOI: 10.1061/(ASCE)0733-9429(2002)128:12(1087).

Lantz, W., Crookston, B. M., and Palermo, M. 2020. "Flood Infrastructure: Localized Scour at Piano Key Weirs." *Dam Safety 2020: Conference Proceedings*. Association of State Dam Safety Officials. Lexington, KY.

Laugier, F., Vermeulen, J., and Lefebvre, V. 2013. "Overview of Piano Key Weirs experience developed at EDF during the past few years." *Labyrinth and Piano Key Weirs II: PKW 2013*, 213-226. London, UK:Taylor and Francis Group.

Laursen, E. M. 1952. "Observations on the Nature of Scour." In *Proc., 5th Hydraulics Conf*., *Bulletin,*179-197. Iowa City, IA: Univ. of Iowa.

López-Soto, J., Wibowo, J., and Molina-Bas, O. 2016. "Cost Reduction in Dam Infrastructure Using Arced Labyrinth Spillways." *Construction Research Congress 2016*. San Juan, Puerto Rico. DOI: 10.1061/9780784479827.066.

Machiels, O., Pirotton, M., Pierre, A., Dewals, B., and Erpicum, S. 2014. "Experimental parametric study and design of Piano Key Weirs." *J. Hydraul. Res*. 52(3). 326–335. DOI: 10.1080/00221686.2013.875070.

Marsooli, R., Lin, N., Emanuel, K., and Feng, K. 2019. "Climate change exacerbates hurricane flood hazards along US Atlantic and Gulf Coasts in spatially varying patterns." *Nature Communications*. 10(1). 3785. DOI: 10.1038/s41467-019-11755-z.

Mason, P. J., and Arumugam, K. 1985. “Free Jet Scour Below Dams and Flip Buckets.” *J. Hydraul. Eng*. 111(2). 220–235. DOI: 10.1061/(ASCE)0733-9429(1985)111:2(220).

Meftah, B. M., and Mossa, M. 2020. “New Approach to Predicting Local Scour Downstream of Grade-Control Structure.” *J. Hydraul. Eng*. 146(2). DOI: 10.1061/(ASCE)HY.1943-7900.0001649.

Microsonic. 2021. “mic+ 130/IU/TC.” *mic+ ultrasonic sensors*. Accessed: Mar. 4, 2021. <https://www.microsonic.de/en/distance-sensors/cylindrical/micplus/standard-sensors/standard-sensors/micplus130iutc.htm>

Nasrollahi, A., Ghodsian, M., and Neyshabour, S. A. A. S. 2008. “Local Scour at Permeable Spur Dikes.” *Journal of Applied Sciences*. 8(19). 3398–3406. DOI: 10.3923/jas.2008.3398.3406.

National Weather Service (NWS), National Oceanic and Atmospheric Administration (NOAA). 2020. “NWS Preliminary US Flood Fatality Statistics.” Accessed: Jan. 25, 2020. <https://www.weather.gov/arx/usflood>

Noseda, M., Stojnic, I., Pfister, M., and Schleiss, A. J. 2019. “Upstream Erosion and Sediment Passage at Piano Key Weirs.” *J. Hydraul. Eng*. 145(8). 04019029. DOI: 10.1061/(ASCE)HY.1943-7900.0001616.

Novak, P., Moffat, A. I. B., Nalluri, C., and Narayanan, R. 1995. *Hydraulic Structures*. 4th Ed. Milton Park, Abingdon, Oxon: E & FN Spon.

Pagliara, S., Amidei, M., and Hager, W. H. 2008. “Hydraulics of 3D Plunge Pool Scour.” *J. Hydraul. Eng*. 134(9). 1275–1284. DOI: 10.1061/(ASCE)0733-9429(2008)134:9(1275).

Palermo, M., Bombardelli, F. A., and Pagliara, S. 2018. "From Developing to Developed Phase in the Scour Evolution Due to Vertical and Sub-vertical Plunging Jets: New Experiments and Theory." *7th International Symposium on Hydraulic Structures*. Aachen, Germany. DOI: 10.15142/T3ZH2Z.

Palermo, M., Crookston, B., and Pagliara, S. 2020. "Analysis of Equilibrium Morphologies Downstream of a PK Weir Structure." *World Environmental and Water Resources Congress 2020*, American Society of Civil Engineers (ASCE). 43–51. DOI: 10.1061/9780784482971.005.

Palermo, M., Pagliara, S., and Bombardelli, F. A. 2020b. "Theoretical Approach for Shear-Stress Estimation at 2D Equilibrium Scour Holes in Granular Material due to Subvertical Plunging Jets." *J. Hydraul. Eng*. 146(4). 0402009. DOI: 10.1061/(ASCE)HY.1943-7900.0001703.

Pralong, J., Vermeulen, J., Blancher, B. Laugier, F., Erpicum, S., Machiels, O., Pirotton, M., Boillat, J. L., Ribeiro, M.L. Schleiss, A. J. 2011. "A naming convention for the Piano Key Weirs geometrical parameters." *Labyrinth and Piano Key Weirs: PKW 2011*. 271-296. London, UK: Taylor and Francis Group.

Peterka, J. 1958. *Hydraulic Design of Stilling Basins and Energy Dissipators.* Bureau of Reclamation: Denver, CO.

Pfister, M., Jüstrich, S., and Schleiss, A. 2017. "Toe-scour formation at Piano Key Weirs." *Labyrinth and Piano Key Weirs III – PKW 2017*. 147–156. London, UK:Taylor and Francis Group.

Ribeiro, M. L., Pfister, M., Schleiss, A. J., and Boillat, J. L. 2012. “Hydraulic design of A-Type Piano Key Weirs.” *J. Hydraul. Res*. 50(4). 400–408. DOI: 10.1080/00221686.2012.695041.

Sarkar, A., and Dey, S. 2005. “Scour downstream of aprons caused by sluices.” *Proc., Inst. Civ. Eng., Water Management J*., London, 158(June), 55–64.

Schleiss, A. J. 2011. “From Labyrinth to Piano Key Weirs – A historical review.” *Labyrinth and Piano Key Weirs: PKW 2011*. 3-16. London, UK: Taylor and Francis Group.

Schoklitsch, A. 1932. *Kolkbildung unter Uberfallstrahlen.* 343. Germany: Wasserwirtschaft.

Thompson, P., and Kilgore, R. 2006. “Hydraulic Design of Energy Dissipators for Culverts and Channels.” Federal Highway Administration. Washington D.C.: National Highway Institute.

Urban and Environmental Engineering (UEE). (2021). "World register of piano key weirs prototypes." *Liege Universite* Accessed: March 11, 2021. <https://www.uee.uliege.be/cms/c_5026433/en/world-register-of-piano-key-weirs-prototypes>

United States Department of Agriculture (USDA). 1959. “The SAF Stilling Basin.” Washington D.C.: U.S. Government Printing Office.

Vischer, D. L., and Hager, W. H. 1995. *Energy Dissipators: IAHR Hydraulic Structures Design Manuals 9.* Milton Park, Abingdon, Oxon: Taylor and Francis.

Wang, L., Melville, B. W., Whittaker, C. N., and Guan, D. 2019. “Scour Estimation Downstream of Submerged Weirs.” *J. Hydraul. Eng*. 145(12). 06019016. DOI: 10.1061/(ASCE)HY.1943-7900.0001654.

Yazdi, A. M., Hoseini, S. A., Nazari, S., and Amanian, N. 2021. “Effects of weir geometry on scour development in the downstream of Piano Key Weirs.” *Water Supply*. 21(1). 289–298. DOI: 10.2166/ws.2020.272.

Zehe, E., Becker, B., Bardossy, A., and Plate, E. 2005. “Uncertainty of simulated catchment runoff response in the presence of threshold processes: Role of initial soil moisture and precipitation.” *J. Hydrol*. 315(1-4). 183–202. DOI: 10.1016/j.jhydrol.2005.03.038.

Zhang, G., Valero, D., Bung, D. B., and Chanson, H. 2018. “On the estimation of free-surface turbulence using ultrasonic sensors.” *Flow Measurement and Instrumentation*. 60. 171–184. DOI: 10.1016/j.flowmeasinst.2018.02.009

APPENDICES

Appendix A – USU Custom MATLAB Script

Variables that need to change for this file to work

```
clear all
clc
close all




Date = "05/29/2020"; %MM/DD/YYYY
DSBaseVal = 749; % D.S. Ultra Sonic Base Value in mm
HtOP = .1248; % From SPreadsheet Pt guage reading used to calculate
ZMaxMeas = .782; %in meters
% USBaseVal = 313; %Upstream Ultra Sonic Base in mm %Commented Out 12/16/20
% need to determine the U.S. base for upstream
t = 6*60;
Apron = 1.5;
QTab = 150;
Q = 150.01;% From spreadsheet
TW = 14;
GS = 'Three Quarter Gravel';
AS= '1.5P';
FR = '150';
TWC = 'Low';
SF1 = 'Figures';
SF2 = 'PLY Files';
SF3 = 'Ultra Sonic Data';
SF4 = 'Data Validation';
SF5 = 'Variables';
DS = 'D.S';
US = 'U.S';
ftype1 = '*.ply';
ftype2 = '*.txt';
Fig1Name = '\1.5_150_14_3Dgray_T.png';
Fig4Name = '\1.5_150_14_3Dcolor_T.png';
Fig3Name = '\1.5_150_14_Profiles_T.png';
Fig3 = '';
VarName = '\1.5_150_14T.mat';
D50 = .013; %Meters
P = .4186; %
Ht = HtOP*P;
Z = .754-ZMaxMeas+(.1*(-1)); %Approx. scour depth
A = Apron*P+.0221;
outs = .1; %Stdev for averaging, 1 for 150, 2 for 600
myz = .128; %minimum scour depth y location


%Permanent Values
Pb = (43*2.54)/100;
```

```
Width = (6.542*12*2.54)/100;
g = 9.80665;
```

Creating directories and reading in tables.

```
d = fullfile(pwd,'Gravel Size', GS,AS,FR,TWC,SF2,ftype1);
fig = fullfile(pwd,'Gravel Size',GS,AS,FR,TWC,SF1);
var = fullfile(pwd,'Gravel Size',GS,AS,FR,TWC,SF5);
twd = fullfile(pwd,'Gravel Size', GS,AS,FR,TWC,SF3,DS,ftype2);
hd = fullfile(pwd,'Gravel Size', GS,AS,FR,TWC,SF3,US,ftype2);
```

Calling Functions

```
[Zmax,comb600e, aveval, avemaxval,f1,f3,f4,Xmax] = PLYProcess(d,Z,A,outs,Fig3)%,DVd,myz) % Look at
the data validation location
[L,Lvals] = Length(avemaxval,A);
twd = fullfile(pwd,'Gravel Size', GS,AS,FR,TWC,SF3,DS,ftype2);
[TWVal,Hd] = TWFun(twd,DSBaseVal,Q,Width,g);
[USHt,USHu] = HtFun(hd,USBaseVal,Q,P,g,Pb,Width) % 12/16/20 Just Using Pt Gage for
upstream head values
```

Calculations

```
%Ultra Sonic and Pt Guage Percent Difference
Hu = Ht+P;
TWVal = .099;
Hd = ((((Q*.001)/(TWVal*Width))^2)/(2*g))+TWVal;
Res = (Hu-Hd)/Hu;
ZdL = Zmax/L;
ZdX = Zmax/Xmax;
HdH = Hd/Hu;
XdZ = Xmax/Zmax;
Q = QTab;
```

Importing scour table and adding to table and creating graphs

```
ScourTable = readtable("ScourTable.txt");
```

!!STOP!! and confirm that data looks good before proceeding

Saving Figures and Exporting Values

```
T = table(Date,P,D50,Apron,Q,TW,TWVal,t,Zmax,L,Xmax,Ht,Hu,Hd,HtOP,Res,ZdX,HdH,XdZ,ZdL);
ScourTable9 = [ScourTable9;T]
```

```
writetable(T,'ScourTable9','Delimiter',',');
writetable(ScourTable9,'ScourTable9','Delimiter',',');
save([var,VarName],'Date','P','D50','Apron','Q','TW','TWVal','t','Zmax','L','Xmax','Ht','Hu','Hd',
'HtOP',...
    'Res','ZdX','HdH','XdZ','ZdL','USHu','USHt','Lvals','comb600e','aveval','avemaxval')
save([var,VarName],'Date','P','D50','Apron','Q','TW','TWVal','t','Zmax','L','Xmax','Ht','Hu','Hd',
'HtOP',...
    'Res','ZdX','HdH','XdZ','ZdL','Lvals','comb600e','aveval','avemaxval')
saveas(f1,[fig, Fig1Name]);
saveas(f4,[fig, Fig4Name]);
saveas(f3,[fig, Fig3Name]);
```

Length Function

```
function [L,Lvals] = Length(avemaxval,Apron)
    if Apron == 0
        zvals = avemaxval(:,2);
        [Zmax,Row] = min(zvals);
        Xmax = avemaxval(Row,1);
        %         Xmax = aveval(Row,1);
        k = 1;
        Lvals = [];
        L1 = [];
        L2 =[];
        if avemaxval(1,:) == 0
            Lvals(1,:) = 0;
        else
            for j = 1:length(avemaxval)
                if avemaxval(j,1) > Xmax && avemaxval(j,1) < 4.8
                    if avemaxval(j,2) >= -.01 && avemaxval(j,2) <= .01
                        %Need to fix change the average vals for the steps to 500
                        Lvals(k,:) = avemaxval(j,:);
                        k = k+1;
                    end
                end
            end
            if isempty(Lvals) == 0
                L1 = (Lvals(1,1)+Lvals(2,1))/2;
            end

            if isempty(Lvals) == 1
                for j = 1:length(avemaxval)
                    if avemaxval(j,1) > Xmax && avemaxval(j,1) < 4.8
                        if avemaxval(j,2) >= -.1 && avemaxval(j,2) <= 0
```

```
                            %Need to fix change the average vals for the steps to 500
                            Lvals(k,:) = avemaxval(j,:);
                            k = k+1;
                        end
                    end
                end
                oneInEvery5Lvals = Lvals(1:5:end,:);
                for i = 1:length(oneInEvery5Lvals)-1
                    rateOfChange(i,1) = (oneInEvery5Lvals(i+1,2)-
oneInEvery5Lvals(i,2))/(oneInEvery5Lvals(i+1,1)-oneInEvery5Lvals(i,1));
                end
                for i = 1:length(rateOfChange)
                    if rateOfChange(i,1) < 0.02
                        break
                    else
                        signFlipRow = i;
                    end
                end
                signFlipRow = signFlipRow+1;
                rowinLvals = (signFlipRow*5)-4;
                L2 = Lvals(rowinLvals,1);
            end
        end


    elseif Apron > 0

        zvals = avemaxval(:,2);
        [Zmax,Row] = min(zvals);
        Xmax = avemaxval(Row,1);
        k = 1;
        Lvals = [];
        L1 = [];
        L2 =[];
        if avemaxval(1,:) == 0
            Lvals(1,:) = 0;
        else
            for j = 1:length(avemaxval)
                if avemaxval(j,1) > Xmax && avemaxval(j,1) < 4.8
                    if avemaxval(j,2) >= -.01 && avemaxval(j,2) <= .01
                        %Need to fix change the average vals for the steps to 500
                        Lvals(k,:) = avemaxval(j,:);
                        k = k+1;
                    end
                end
            end
            if isempty(Lvals) == 0
                L1 = (Lvals(1,1)+Lvals(2,1))/2;
```

```
            end

            if isempty(Lvals) == 1
                for j = 1:length(avemaxval)
                    if avemaxval(j,1) > Xmax && avemaxval(j,1) < 4.8
                        if avemaxval(j,2) >= -.1 && avemaxval(j,2) <= 0
                            %Need to fix change the average vals for the steps to 500
                            Lvals(k,:) = avemaxval(j,:);
                            k = k+1;
                        end
                    end
                end
                oneInEvery5Lvals = Lvals(1:5:end,:);
                for i = 1:length(oneInEvery5Lvals)-1
                    rateOfChange(i,1) = (oneInEvery5Lvals(i+1,2)-
oneInEvery5Lvals(i,2))/(oneInEvery5Lvals(i+1,1)-oneInEvery5Lvals(i,1));
                end
                for i = 1:length(rateOfChange)
                    if rateOfChange(i,1) < 0.02
                        break
                    else
                        signFlipRow = i;
                    end
                end
                signFlipRow = signFlipRow+1;
                rowinLvals = (signFlipRow*5)-4;
                L2 = Lvals(rowinLvals,1);


            end
        end
    end
end
```

TW Function

```
function [TWVal,Hd] = TWFun(twd,base,Q,Width,g)
    USfiles = dir(twd);
    base = base; % in millimeters
    for i = 1:length(USfiles)
        ffile = fullfile(USfiles(i).folder,USfiles(i).name);
        f = readmatrix(ffile);
        avetw(i,1) = nanmean(f(:,3));
    end
    avetw = nanmean(avetw);
    TWVal = (base-avetw)/1000;
    Hd = ((((Q*.001)/(TWVal*Width))^2)/(2*g))+TWVal;
end
```

Total Head Function For Ultra Sonic

```
function [Ht,Hu] = HtFun(hd,base,Q,P,g,Pb,Width)
```

```
    USfiles = dir(hd);
    base = base; % in millimeters
    for i = 1:length(USfiles)
        ffile = fullfile(USfiles(i).folder,USfiles(i).name);
        f = readmatrix(ffile);
        avetw(i,1) = nanmean(f(:,3));
    end
    avetw = mean(avetw);
    ht = (base - avetw)/1000;
    V = (Q*.001)/((ht+P+Pb)*Width);
    VH = ((V^2)/(2*g));
    Ht = VH+ht;
    Hu = Ht+P;
end
```

PolyProcess Function File

```
function [Zmax,comb600e, aveval, avemaxval,f1,f3,f4,Xmaximum] =
PLYProcess(directory,ApproxMaxScourDepth,Apron,outs, Fig3)%,DVd,myz) %commented out 12/16/2020
    f = fullfile(directory);
    files600 = dir(f);


    %Keep the following values in meters.
    MaxScourDepth = ApproxMaxScourDepth;
    MaxDuneHeight = .1;
    LocationPlexiWall = 0.05;
    LocationFarWall = 1.9;
    LocationFound = 0;
    Weirx = .25;
    Weirz = .05;
    A = Apron;


    % % Titles for the figure using the flow rate and tail water.
    %Fig1Title = '3D Color Map for Q = 150 (L/s) and TW = 15.6 (cm)';
    Fig1Title = 'General Scour Formation';
    Fig1Name = '3D_2_300_14_gray.png';
    Fig4Name = '3D_2_300_14_color.png';
    Fig2Title = 'Average Scour Depth Profile Q = 600 L/s and TW = 42.6 cm';
    Fig3Title = Fig3;


    %This loops creates fields and populates them with values from the file
    %name such as flowrate (Q), tailwater depth (TW), etc.
    for i = 1:length(files600)
        C = strsplit(files600(i).name,'_');
        C(6) = [];
        C = str2double(C);
        [files600(i).Q] = C(1);
```

```
        [files600(i).TW] = C(2);
        [files600(i).Y] = C(3)-8;
        [files600(i).X] = C(4);
        if C(5) == 6 || C(5) == 21.3
            [files600(i).Z] = -C(5);
        else
            [files600(i).Z] = C(5);
        end


    end
    %This organizes the structures into camera locations along the X axis of
    %the flume
    T = struct2table(files600);
    sortedfiles = sortrows(T, [9,10]);
    files600 = table2struct(sortedfiles);




    for i = 1:length(files600)
        fname = fullfile(files600(i).folder,files600(i).name);
        pc = pcread(fname);
        pc = pcdenoise(pc);
        gridStep = 0.01;
        pc = pcdownsample(pc,'gridAverage',gridStep);
        files600(i).xyzne = reshape(pc.Location, [], 3);
        files600(i).xyzne = sortrows(files600(i).xyzne, 1);


        files600(i).xyz(:,1) = (files600(i).X/100) + files600(i).xyzne(:,1);
        files600(i).xyz(:,2) = ((files600(i).Y/100)-.004589) - files600(i).xyzne(:,2);%.004589 is
a correction
        files600(i).xyz(:,3) = (files600(i).Z/100) + files600(i).xyzne(:,3);


           l = length(files600(i).xyz);
        for j = 1: length(files600(i).xyz)
            %Trying to get rid of the weir without getting rid of anything else
            if files600(i).xyz(j,2) <= Weirx && files600(i).xyz(j,3) >= Weirz
                files600(i).xyz(j,:) = NaN;
            end
            %Rough cuts trying to denoise the image
            if files600(i).xyz(j,3) < MaxScourDepth
                files600(i).xyz(j,:) = NaN;
            end
            if files600(i).xyz(j,3) > MaxDuneHeight
                files600(i).xyz(j,:) = NaN;
```

```
            end
            %Getting rid of the plexiglass sid wall
            if files600(i).xyz(j,1) < LocationPlexiWall
                files600(i).xyz(j,:) = NaN;
            end
            %Getting rid of the foundation of the wier
            if files600(i).xyz(j,2) < LocationFound
                files600(i).xyz(j,:) = NaN;
            end
            if files600(i).xyz(j,2) < A
                files600(i).xyz(j,3) = 0;
            end
            %Getting rid of values after substrate bed
            if files600(i).xyz(j,2) > 4.7
                files600(i).xyz(j,:) = NaN;
            end
            %Getting rid of the far wall of the flume.
            if files600(i).xyz(j,1) > LocationFarWall
                files600(i).xyz(j,:) = NaN;
            end
        end
    end
    %finding average along flume length
    comb600 = [];
    for i =1:length(files600)
        comb600 = [comb600;files600(i).xyz];
    end
    comb600 = sortrows(comb600, 2);
    xvals = [];
    xvals = comb600(:,2);
    xmax = max(xvals);
    xmin = min(xvals);
    xstep = (xmax-xmin)/500;
    xint = xmin;


    zoutl = outs;
    k = 1;
    l = 1;
    comb600e = [];
    while ~isnan(comb600(k,1))
        %getting data
        xintstep = xint+xstep;
        j = 1;
        for i = k:length(comb600)
            if comb600(i,2) >= xint && comb600(i,2) < xintstep
                xdata(j,:) = comb600(i,:);
                j = j+1;
```

```
            else
                xdata(j,:) = comb600(i,:);
                k = i+1; %+1;
                break
            end
        end

        Q1 = prctile(xdata,25,'all');
        Q3 = prctile(xdata,75,'all');
        r = Q3-Q1;
        UL = Q3+(zoutl*r);
        LL = Q1-(zoutl*r);
        H = size(xdata,1);
        for i = 1:H
            if xdata(i,3) < LL || xdata(i,3) > UL
                xdata(i,:) = NaN;
            end
        end
        zmean = nanmean(xdata(:,3));
        xmean = nanmean(xdata(:,2));
        while ~isnan(comb600(k,1))
            aveval(l,1) = xmean;
            aveval(l,2) = zmean;
            l = l+1;
            break
        end
        comb600e = [comb600e;xdata];
        xdata = [];
        xint = xintstep; %Added
    end
    comb600e = sort(comb600e,[3],"ascend");


    comb600x = comb600e(:,2);
    comb600y = comb600e(:,1);
    comb600z = comb600e(:,3);

    for i = 1:length(comb600z)
        zrow = sort(comb600z);
        MinZ = zrow(i);
        [Row,Col] = find(comb600z==MinZ);
        yval = comb600y(Row,1);
        for j = 1:length(yval)
            if yval(j) > .25 && yval(j) < 1.75
                break
            end
        end
        if yval(j) > .25 && yval(j) < 1.75
```

```
            break
        end
    end

    yval = yval(j);
```

3D Scour Plot

```
    f1 = figure;
    set(f1,'Units','Inches','InnerPosition', [5 5 6 3]);
    scatcol = scatter3(comb600x,comb600y,comb600z, 5, comb600z, '.');
    hold on
    colormap(flipud('gray'));
    colorbar;
    xlabel('$x$ (m)','Interpreter','LaTex')
    ylabel('$y$ (m)','Interpreter','LaTex')
    zlabel('$z$ (m)','Interpreter','LaTex')
    axis equal;
    axis([0 3.75 0 2 -1.10 .5]); %3.75
    grid on;
    grid minor;
    view(45,30);
    figure(f1)


    % 3D Scour Plot
    f4 = figure;
    set(f4,'Units','Inches','InnerPosition', [5 5 6 3]);
    scat = scatter3(comb600x,comb600y,comb600z, 5, comb600z, '.');
    hold on
    colormap(flipud(jet));
    colorbar;
    xlabel('$x$ (m)','Interpreter','LaTex', 'FontSize', 12)
    ylabel('$y$ (m)','Interpreter','LaTex', 'FontSize', 12)
    zlabel('$z$ (m)','Interpreter','LaTex', 'FontSize', 12)
    axis equal;
    axis([0 3.75 0 2 -1.10 .5]);
    grid on;
    grid minor;
    view(45,30);
    figure(f4)
```

Average of points along the Max Scour Proile

```
    k =1;
    comb600e = sortrows(comb600e, 2);
    while ~isnan(comb600e(k,1))
        for j = 1: length(comb600e)
            if comb600e(j,1) > yval-.01 && comb600e(j,1) < yval+.01
```

```
            zdata(j,:) = comb600e(j,:);
            if j == length(comb600e)
                break
            end
        else
            zdata(j,1:3) = NaN;
            k = j;
            if j == length(comb600e)
                break
            end
        end
    end
    if j == length(comb600e)
        break
    end
end


zdata = sortrows(zdata, 2);
xmax = max(zdata(:,2));
xmin = min(zdata(:,2));
xstep = (xmax-xmin)/500;
xint = xmin;
k = 1;
l = 1;
zm = [];
while ~isnan(zdata(k,1))
    %getting data
    xintstep = xint+xstep; %Added
    j = 1;
    for i = k:length(zdata)
        if zdata(i,2) >= xint && zdata(i,2) < xintstep %comb600(i,2) == comb600(i+1,2)
            data(j,:) = zdata(i,:);
            j = j+1;
        else
            data(j,1:3) = NaN; %added
            k = i; %+1;
            break
        end
    end


    if isnan(data(:,:))
        zmean = NaN;
        xmean = NaN;
    else
        zmean = nanmean(data(:,3));
        xmean = nanmean(data(:,2));
```

```
        end
        while ~isnan(zdata(k,1))
            avemaxval(l,1) = xmean;
            avemaxval(l,2) = zmean;
            l = l+1;
            break
        end
        zm = [zm;data];
        data = [];
        xint = xintstep; %Added
    end
    avemaxval = sortrows(avemaxval, 1);
    if max(avemaxval,1) < 3.75
        avemaxval = [avemaxval;3.75,0];
        aveval = [aveval;3.75,0];
    end
    avemaxval = sortrows(avemaxval, 1);
```

Data Validation

```
%     DataVal = readmatrix(DVd);
%     DVPts(:,1) =DataVal(:,1);
%     DVPts(:,2) =DataVal(:,3);
% %     for i = 1:length(aveval)
% %         if aveval(i,1) < 1.06 & aveval(i:1) > 1.05 %aveval is just x and z coordinates.
% %             MidFlPts(i,:) = aveval(i,:);
% %         end
% %     end
%
%     k =1;
%     comb600e = sortrows(comb600e, 2);
%    % while ~isnan(comb600e(k,1)) 8/3
%         for j = 1: length(comb600e)
%             if comb600e(j,1) > 1.505-.02 && comb600e(j,1) < 1.505
%                 MidFlPt(k,:) = comb600e(j,:);
%                 k = k+1;%Added 8/3
%             else %elseif comb600e(j,1) < yval-.005 && comb600e(j,1) > 1.06
% % %                 zdata(j,1:3) = NaN;
% % %                 k = j;
%             end
%         end


%     zdata = sortrows(zdata, 2);
%     xmax = max(zdata(:,2));
%     xmin = min(zdata(:,2));
%     xstep = (xmax-xmin)/500;
%     xint = xmin;
%     k = 1;
```

```
%     l = 1;
%     zm = [];
%     %comb600e = NaN(size(comb600));
%     %xdata = NaN(1000,3);
%     while ~isnan(zdata(k,1))
%         %getting data
%         xintstep = xint+xstep; %Added
%         j = 1;
%         for i = k:length(zdata)
%             if zdata(i,2) >= xint && zdata(i,2) < xintstep %comb600(i,2) == comb600(i+1,2)
%                 data(j,:) = zdata(i,:);
%                 j = j+1;
%             else
%                 data(j,1:3) = NaN; %added
%                 k = i; %+1;
%                 break
%             end
%         end
%         %     zmean = mean(xdata(:,3));
%         %     zstd = std(xdata(:,3));
%         %     H = size(xdata,1);
%         %     for i = 1:H
%         %         if xdata(i,3) < zmean-(.125*zstd) || xdata(i,3) > zmean+(.125*zstd)
%         %             xdata(i,:) = NaN;
%         %         end
%         %     end
%         if isnan(data(:,:))
%             zmean = NaN;
%             xmean = NaN;
%         else
%             zmean = nanmean(data(:,3));
%             xmean = nanmean(data(:,2));
%         end
%         while ~isnan(zdata(k,1))
%             MidFlPt(l,1) = xmean;
%             MidFlPt(l,2) = zmean;
%             l = l+1;
%             break
%         end
%         zm = [zm;data];
%         data = [];
%         xint = xintstep; %Added
%     end
%
%     if max(MidFlPt,1) < 3.75
%         MidFlPt = [MidFlPt;3.75,0];
%     end
%     MidFlPt = sortrows(MidFlPt, 1);
```

Min Scour

```
%    x = comb600x(Row,1);
%    j = 1;
%    for i = 1:length(comb600e)
%        if comb600e(i,2) < x+.01 && comb600e(i,2) > x-.01
%            xvalues(j,:) = comb600e(i,:);
%            j = j+1;
%        end
%    end
%    zzvalues = xvalues(:,3);
%    [zmin,row] = max(zzvalues);
%    yzmin = xvalues(row,1);
%    [nrow,ncol] = find(comb600y==yzmin);
%    yzvalue = comb600e(nrow,1);
%    for i = 1:length(aveval)
%        if aveval(i,2) < xzmin+.05 && aveval(i:2) > xzmin-.05
%            minsc(i,:) = aveval(i,:);
%        end
%    end


%     yzvalue = myz;
%     k =1;
%     comb600e = sortrows(comb600e, 2);
%     while ~isnan(comb600e(k,1))
%         for j = 1: length(comb600e)
%             if comb600e(j,1) > yzvalue-.005 && comb600e(j,1) < yzvalue+.005
%                 zdata(j,:) = comb600e(j,:);
%             else %elseif comb600e(j,1) < yval-.005 && comb600e(j,1) > 1.06
%                 zdata(j,1:3) = NaN;
%                 k = j;
%             end
%         end
%     end
%
%     zdata = sortrows(zdata, 2);
%     xmax = max(zdata(:,2));
%     xmin = min(zdata(:,2));
%     xstep = (xmax-xmin)/500;
%     xint = xmin;
%     k = 1;
%     l = 1;
%     zm = [];
%     %comb600e = NaN(size(comb600));
%     %xdata = NaN(1000,3);
%     while ~isnan(zdata(k,1))
%         %getting data
%         xintstep = xint+xstep; %Added
```

```
%         j = 1;
%         for i = k:length(zdata)
%             if zdata(i,2) >= xint && zdata(i,2) < xintstep %comb600(i,2) == comb600(i+1,2)
%                 data(j,:) = zdata(i,:);
%                 j = j+1;
%             else
%                 data(j,1:3) = NaN; %added
%                 k = i; %+1;
%                 break
%             end
%         end
%     %     zmean = mean(xdata(:,3));
%     %     zstd = std(xdata(:,3));
%     %     H = size(xdata,1);
%     %     for i = 1:H
%     %         if xdata(i,3) < zmean-(.125*zstd) || xdata(i,3) > zmean+(.125*zstd)
%     %             xdata(i,:) = NaN;
%     %         end
%     %     end
%         if isnan(data(:,:))
%             zmean = NaN;
%             xmean = NaN;
%         else
%             zmean = nanmean(data(:,3));
%             xmean = nanmean(data(:,2));
%         end
%         while ~isnan(zdata(k,1))
%             minz(l,1) = xmean;
%             minz(l,2) = zmean;
%             l = l+1;
%             break
%         end
%         zm = [zm;data];
%         data = [];
%         xint = xintstep; %Added
%     end
%
%     if max(minz,1) < 3.75
%         minz = [minz;3.75,0];
%     end
%     minz = sortrows(minz, 1);
```

Plotting

```
    f3 = figure;
    maxscour = plot(avemaxval(:,1),avemaxval(:,2),'b');% ,'.','MarkerEdgeColor','k',...
                % 'MarkerFaceColor','k');
    hold on;
    title(Fig3Title,'Interpreter','LaTex', 'FontSize', 12);
    xlabel('$x$ (m)','Interpreter','LaTex');
```

```
    ylabel('$z$ (m)','Interpreter','LaTex');
    box on;
    axis equal;
    axis([0 3.75 -1.1 .5])
    grid on;
    grid minor;
    figure(f3);


    [Zmax, MRow] = min(avemaxval(:,2));
    Xmaximum = avemaxval(MRow,1);
    if A > 0
        Xmaximum = Xmaximum - A;
    end
end
```

Appendix B – Flume Design Drawings

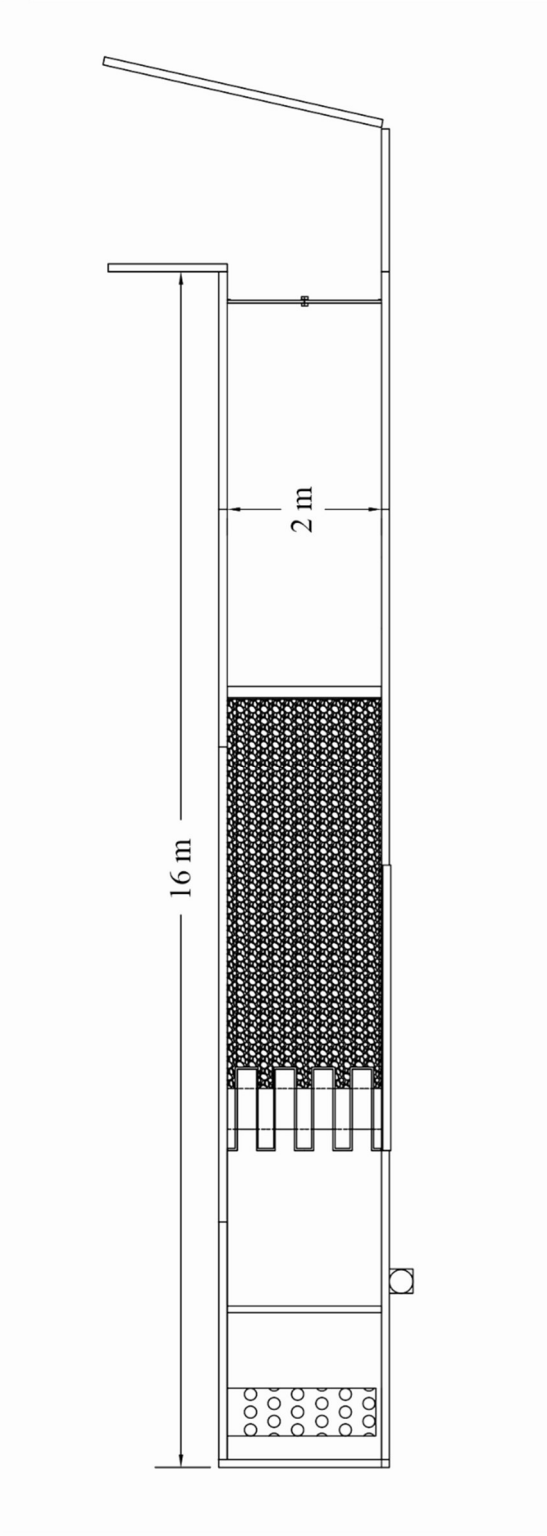

Fig. B1. Flume plan view dimensions.

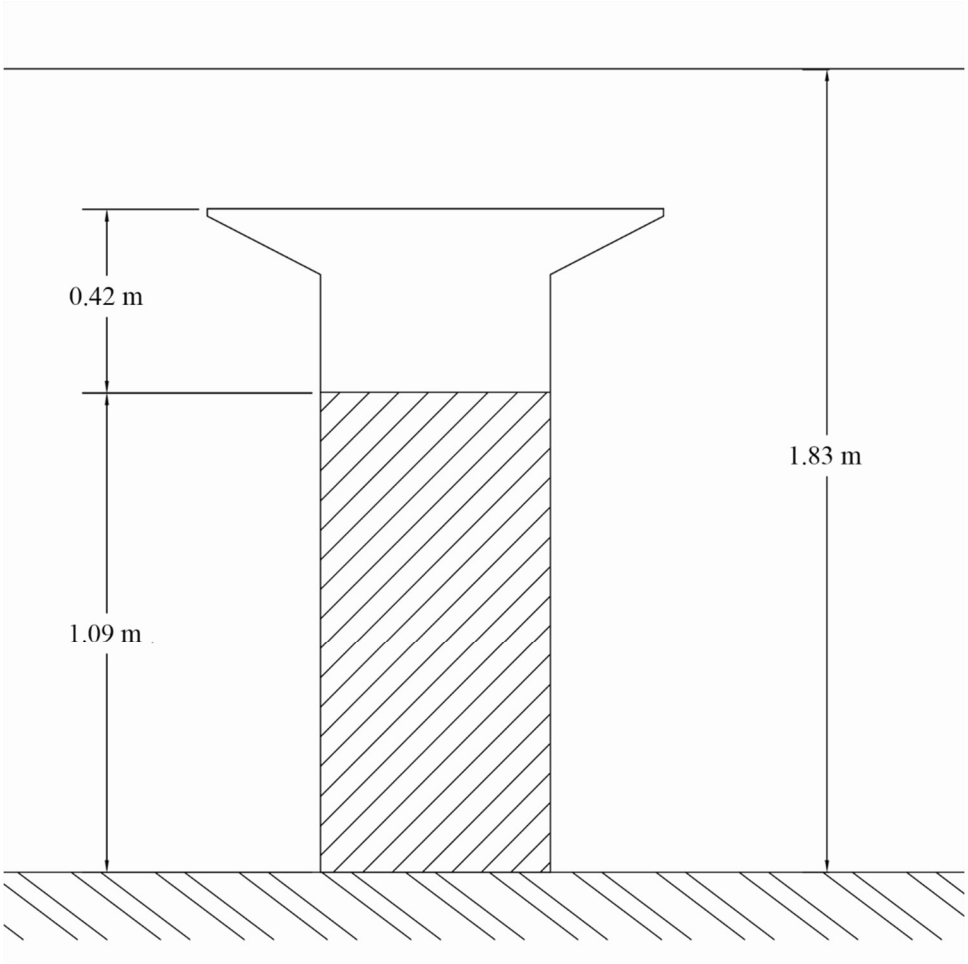

Fig. B2. Profile view of flume with dimensions.

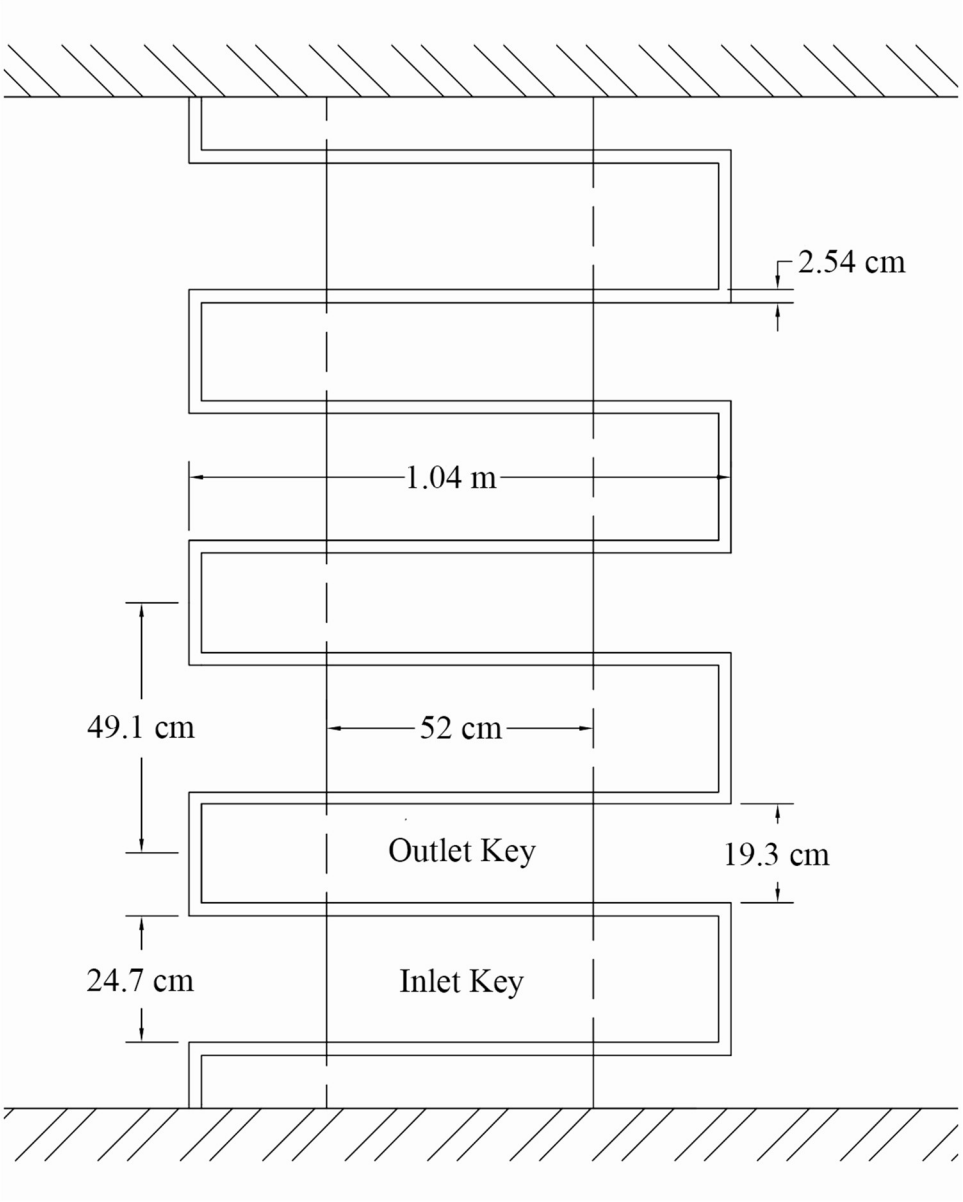

Fig. B3. Schematic of PK weir with dimensions.